Genes to Cells

Herbal drug ninjin'yoeito accelerates myelopoiesis but not erythropoiesis *in vitro*

Tomoko Inoue[1,2†], Kasem Kulkeaw[1†], Kanitta Muennu[1,3,4†], Yuka Tanaka[5,6], Yoichi Nakanishi[6] and Daisuke Sugiyama[1*]

[1]*Department of Research and Development of Next Generation Medicine, Faculty of Medical Sciences, Kyushu University, 3-1-1, Maidashi, Higashi-Ku, Fukuoka 812-8582, Japan*
[2]*Department of Medicine and Biosystemic Science, Graduate School of Medical Sciences, Kyushu University, 3-1-1, Maidashi, Higashi-Ku, Fukuoka 812-8582, Japan*
[3]*Thalassemia Research Center, Institute of Molecular Biosciences, Mahidol University, 25/25, Putthamonthon Sai 4 Rd. Salaya, Putthamonthon, 73170 Nakron Pratom, Thailand*
[4]*Faculty of Medical Technology, Prince of Songkla University, 15 Kanjanavanit Rd. Hat Yai, Songkhla, Thailand*
[5]*Department of Cell Biology, Faculty of Medicine, Fukuoka University, 7-45-1, Nanakuma, Jonan-ku, Fukuoka 814-0180, Japan*
[6]*Center for Clinical and Translational Research, Kyushu University Hospital, 3-1-1, Maidashi, Higashi-Ku, Fukuoka 812-8582, Japan*

Some Kampo medicines that are herbal and traditional in Japan have had beneficial effects when given to patients with anemia. However, molecular mechanisms underlying their effects are unclear. To address this question, four Kampo medicines used to treat anemia—ninjin'yoeito (NYT), shimotsuto (SMT), juzentaihoto (JTT), and daibofuto (DBT)—were tested separately using *in vitro* cultures of mouse bone marrow mononuclear cells. Among them, NYT was most effective in stimulating cell proliferation and up-regulating *Myc* expression. Flow cytometry analysis indicated that, among hematopoietic components of those cultures, myeloid cells expressing CD45/Mac-1/Gr-1/F4/80 increased in number, but Ter119/CD71 erythroid cells did not. Accordingly, real-time PCR analysis showed up-regulation of the myeloid gene *Pu.1*, whereas the erythroid genes *Gata1* and *Klf1* were down-regulated. Overall, these findings provide molecular evidence that NYT accelerates myelopoiesis but not erythropoiesis *in vitro*.

Introduction

Hematopoiesis is the process whereby functional, mature hematopoietic cells (red blood cells (RBCs), leukocytes, and platelets) are generated from hematopoietic stem cells in bone marrow (BM). Erythropoiesis is one aspect of hematopoiesis in which erythroid progenitors, such as burst forming unit-erythroid (BFU-E) and colony forming unit-erythroid (CFU-E) cells, are initially generated and then give rise to erythroblasts, reticulocytes, and finally RBCs, which contain hemoglobin functioning in oxygen transport (McGrath & Palis 2008). Failure of erythropoiesis results in a shortage of or damage to RBCs and underlies anemia.

Kampo is a Japanese herbal medicine and widely used to treat many kinds of diseases. Among them, the group shimotsuto, primarily in combination with other drugs, has been used clinically as a blood replenishment agent to treat anemia. Ninjin'yoeito (NYT), a member of shimotsuto group, reportedly antagonizes various forms of anemia, including iron-deficiency anemia (Yanagihori *et al.* 1995; Ando 1999), aplastic anemia (Ohmori *et al.* 1993; Miyazaki *et al.* 1994), refractory anemia (Ohmori *et al.* 1992; Nagoshi *et al.* 1993), renal anemia (Takemura 2000), and anemia resulting from anticancer therapies in humans (Motoo *et al.* 2005). In mice, oral administration of NYT improves 5-fluorouracil (5-FU) induced anemic conditions, as evidenced by the assessment of

Communicated by: Yo-ichi Nabeshima
**Correspondence:* ds-mons@yb3.so-net.ne.jp
†Equally contributed.

DOI: 10.1111/gtc.12143

reticulocyte and RBC numbers, hemoglobin and hematocrit levels in peripheral blood, and increases in BFU-E and CFU-E in BM (Takano *et al.* 2009). However, molecular mechanisms underlying NYT's effect have not been clarified in human beings or mice.

To address those mechanisms, we examined the effect of herbal remedies on cell proliferation and hematopoietic differentiation of BM mononuclear cells (MNCs) in mice by testing four Kampo medicines, NYT, SMT, JTT, and DBT, all historically used to treat anemia. We found that one of those, NYT, enhanced cell proliferation and up-regulated *Myc* transcript levels, likely accounting for the enhanced proliferative state. Among hematopoietic cells, NYT did not increase percentage of erythroid cells but rather decreased expression of the erythroid genes *Gata1* and *Klf1*, whereas the number of macrophages and granulocytes in cultures increased, accompanied by up-regulation of *Pu.1* expression.

Results

Hematopoietic cell proliferation in the presence of Kampo medicines

To investigate the effect of Kampo medicines on hematopoietic cell proliferation, we cultured BM MNCs separately with four Kampo medicines—ninjin'yoeito (NYT), daibofuto (DBT), juzentaihoto (JTT), or shimotsuto (SMT) (Table S1 and Fig. S1 in Supporting information)—for 11 days. To evaluate a potential direct effect of Kampo medicines, no cytokines were added to the cultures. Both round-shaped and adherent cells were observed in the negative control at day 11, while NYT treatment resulted in variable sizes of round-shaped cells and significant proliferation of the round cells by day 11 (Fig. 1A). Cells treated with SMT, JTT, or DBT exhibited similar morphological changes but showed fewer round-shaped cells (T. Inoue, K. Kulkeaw and K. Muennu, unpublished data). The total number of viable cells in negative control samples (♦) increased slightly by day 4 ($3.1 \pm 1.4 \times 10^5$ cells) and then decreased at days 8 and 11 ($0.5 \pm 0.03 \times 10^5$ and $0.76 \pm 0.1 \times 10^5$ cells, respectively). By contrast, BM MNCs cultured in the presence of NYT, SMT, or DBT exhibited significantly increased proliferation by day 11 ($P < 0.05$) (Fig. 1B). Specifically, NYT-treated cells (■) showed a slight increase at day 4 ($3.1 \pm 0.9 \times 10^5$ cells) and at day 8 ($3.5 \pm 2.1 \times 10^5$ cells) and then showed a 2.55-fold increase by day 11 ($8.9 \pm 3.3 \times 10^5$ cells). JTT-treated cells (●) showed the same trend: Their numbers were $2.6 \pm 1.0 \times 10^5$ cells at day 4, $2.8 \pm 1.8 \times 10^5$ at day 8, and $4.1 \pm 3.0 \times 10^5$ at day 11. However, compared with the negative control, no significant difference was observed in JTT-treated cells at day 11. By contrast, DBT-treated cells (**x**) decreased in number by day 4 ($2.1 \pm 0.6 \times 10^5$ cells) but then consistently increased at days 8 ($4.5 \pm 2.5 \times 10^5$ cells) and 11 ($5.7 \pm 2.0 \times 10^5$ cells). SMT-treated cells (▲) showed the same trend as DBT-treated cells: Their numbers were $2.4 \pm 0.5 \times 10^5$ at day 4, $3.5 \pm 2.9 \times 10^5$ at day 8, and $4.9 \pm 1.1 \times 10^5$ at day 11 (Fig. 1B).

To assess molecular mechanisms underlying cell proliferation, we used real-time PCR to examine expression of the transcription factor *Myc*, which functions in cell proliferation (Fig. 1C). Regardless of the type of Kampo medicine used, *Myc* expression in cell cultures gradually increased, including that seen in the negative control. DBT- and JTT-treated cultures showed lower *Myc* expression than did the negative control, whereas NYT-treated cells showed the highest *Myc* expression (day 4: 0.52 ± 0.03, day 8: 0.70 ± 0.01 and day 11: 1.64 ± 0.21) among all culture conditions at all time points (Fig. 1C). Particularly at day 11, *Myc* expression in NYT-treated cells increased significantly relative to the negative control (1.64 ± 0.21 versus 0.49 ± 0.12; $P = 0.02$) (Fig. 1C).

NYT consists of 12 component medical plants, such as Japanese Angelica root, Rehmannia root, peony root, atractylodes rhizome, Poroa Sclerotium, ginseng, cinnamon bark, Polygala root, Citrus unshiu peel, Astragalus root, Glycyrrhiza and Schisandra fruit. To determine whether the herbal constituents of NYT act synergistically to stimulate cell proliferation, cultures were treated with individual NYT components and assessed for cell number and *Myc* expression. As shown in Fig. S2 and Fig. 1D, all NYT components except for Poria sclerotium and cinnamon bark enhanced proliferation relative to controls. *Myc* expression increased in the presence of Japanese Angelica root ($P = 0.0005$) and Rehmannia root ($P = 0.0002$) but remained lower than that stimulated by NYT (Fig. 1E), suggesting that NYT components act synergistically and that Japanese Angelica root and Rehmannia root are likely essential NYT components.

NYT does not alter erythropoiesis in bone marrow mononuclear cells

We next examined the effect of NYT on erythroid cell differentiation. Both $CD71^+/Ter119^+$ cells

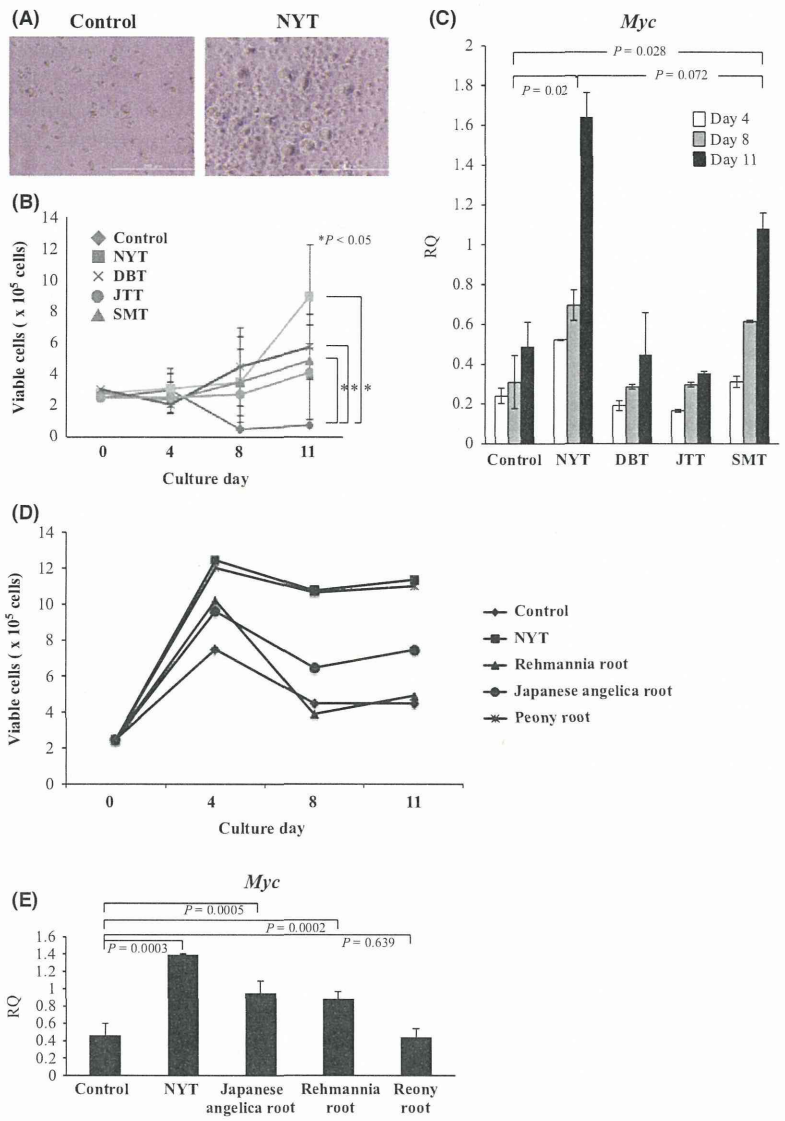

Figure 1 Hematopoietic cell proliferation in the presence of Kampo medicines. (A) Morphology of cells derived from cultured BM MNCs after 11 days of NYT treatment. Shown are phase-contrast images. Scale bars: 200 μm. (B) Total number of viable cells after Kampo medicine treatment. BM MNCs were collected, and viable cells were counted using trypan blue dye after 4, 8, and 11 days. (C), (E) Quantitative real-time PCR analysis of the cell proliferation marker *Myc* at days 4, 8, and 11 (day 11 in E) of cultured BM MNCs. Data are normalized to β-*actin* expression. Student's *t*-test ⋆ was used to calculate statistical significant difference ($P < 0.05$). (D) Total number of viable cells after treatment of NYT and components (Rehmannia root, Japanese Angelica root and Peony root). BM MNCs were collected, and viable cells were counted using trypan blue dye after 4, 8, and 11 days.

representing erythroblasts and $CD71^-/Ter119^+$ cells representing mature erythrocytes were analyzed at days 4, 8, and 11 by flow cytometry. $CD71^-/Ter119^+$ erythrocytes were generated at low efficiency (< 0.6%) in cell culture (Fig. 2A). A significant decrease in the number of $Ter119^+$ cells in NYT-treated culture (1.5 times lower) was observed at day 8, whereas there was no significant difference between $CD71^-/Ter119^+$ cells at days 4 and 11 (Fig. 2B). In agreement, real-time PCR analysis showed that expression of the erythropoietic transcription factor *Gata1* (Whitelaw *et al.* 1990) was

higher in control versus NYT-treated cells (day 4: 0.8 ± 0.16 in controls and 0.147 ± 0.09 in NYT-treated cells; and day 8: 0.419 ± 0.07 in controls and no expression in NYT-treated cells) (Fig. 2C). The transcription factor *Klf1* (Miller & Bieker 1993), whose expression is regulated by Gata1, was detected in controls and NYT-treated cells only on day 4 but not days 8 and 11. No expression of *Klf1* was seen after SMT, JTT, or DBT treatment (T. Inoue, K. Kulkeaw and K. Muennu, unpublished data). These findings indicate that NYT does not accelerate erythroid differentiation.

NYT accelerates myelopoiesis of bone marrow mononuclear cells

To investigate the effect of NYT on leukopoiesis, which consists of myelopoiesis and lymphopoiesis, we examined expression of the common leukocyte antigen CD45, a pan-leukocyte marker, at days 4, 8 (T. Inoue, K. Kulkeaw and K. Muennu, unpublished data), and 11 (Fig. S3A, left in Supporting information) by flow cytometry. Percentage of $CD45^+$ cell was slightly higher in NYT-treated cells (control: 95.1 ± 1.33%, NYT-treated cells: 97.6 ± 0.28%), but the difference was not statistically significant ($P = 0.118$) (Fig. S3A in Supporting information). When leukopoiesis was analyzed by flow cytometry using Mac-1 (CD11b), a marker of macrophages and granulocytes, and B220, a B-lymphocyte marker, NYT-treated BM MNCs differentiated into $CD45^+$/$Mac\text{-}1^+$ cells in numbers 2.23 times greater than controls ($P = 0.002$) (Fig. S3B in Supporting information) and into $CD45^+/Mac\text{-}1^-/B220^+$ B lymphocytes in numbers 3.00 times lower than control ($P = 0.002$) (Fig. S3B in Supporting information) by 11 days in culture. In agreement with the increase in $CD45^+/Mac\text{-}1^+$ cells, real-time PCR analysis showed that expression of *Pu.1 (Spi1)*, which positively regulates generation of macrophages and granulocytes, was higher in NYT-treated cells (1.00 ± 0.001 in controls and 5.55 ± 0.09 in NYT-treated cells) ($P = 0.007$) (Fig. S3C in Supporting information). Also, expression of colony-stimulating factor 1 receptor (*Csf1r*), the receptor for macrophage colony-stimulating factor, was higher in NYT-treated (1.12 ± 0.09 in controls and 1.53 ± 0.08 in NYT-treated cells) ($P = 0.06$) at day 11 (Fig. S3C in Supporting information). Taken together, these findings suggest that the primary effect of NYT on hematopoiesis is to accelerate myelopoiesis.

To investigate NYT activity using purified populations, we removed erythroid cells by sorting $CD45^+$/$Ter119^-$ cells from BM MNCs (Fig. 3A) and then

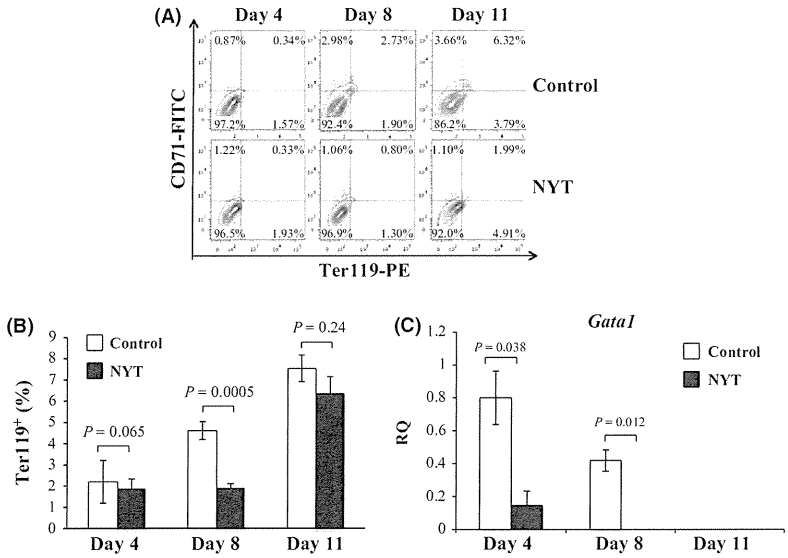

Figure 2 NYT treatment does not alter erythropoiesis. (A) BM MNCs cultured with and without NYT were collected at days 4, 8, and 11, and erythroid differentiation was assessed by flow cytometric analysis of cells stained positive for CD71 and Ter119. The percentage of $Ter119^+$ erythroid cells is shown in (B). (C) Quantitative real-time PCR analysis of the erythroid gene *Gata1* at days 4, 8, and 11. Data were assessed by normalized values to control at day 4.

cultured them in the presence of NYT for 11 days. The total number of cells in the untreated negative control group increased at day 4 ($2.93 \pm 0.11 \times 10^5$ cells) and then decreased at days 8 and 11 ($2.40 \pm 0.84 \times 10^5$ and $2.10 \pm 0.42 \times 10^5$ cells, respectively). By contrast, NYT-treated $CD45^+$ cells showed a 2.4-fold increase in total cell number at day 4 ($4.80 \pm 0.21 \times 10^5$ cells) ($P = 0.007$), decreased at day 8 ($4.20 \pm 0.42 \times 10^5$ cells) ($P = 0.116$), and then increased at day 11 ($6.75 \pm 1.06 \times 10^5$ cells) ($P = 0.029$) (Fig. 3B). Flow cytometric analysis (Fig. 3C) showed that $CD45^+$ cells were more abundant in NYT-treated (94.0 ± 0.46%) versus control (73.7 ± 1.89%) cells ($P = 0.0001$) (Fig. 3C). Among $CD45^+$ cells, the proportion of $Mac\text{-}1^+/F4/80^+$ macrophages differentiated from BM MNC $CD45^+$ cells was 8.05 times higher in NYT-treated than in control cells ($P = 0.01$) (Fig. 3D). Moreover, the proportion of $Mac\text{-}1^+/Gr\text{-}1^+$ granulocytes was 3.41 times higher in NYT-treated than control cells ($P = 7.07 \times 10^{-6}$) (Fig. 3E). Furthermore, real-time PCR analysis showed that expression of *Pu.1* was higher in cultures of NYT-treated compared with control cells (3.15-fold at day 4, 1.28-fold at day 8 and 5.43-fold at day 11) (Fig. 3F). *Csf1r* expression was 8.41 times lower in NYT-treated compared with control cells at day 4, 4.72 times higher at day 8, and 2.66 times higher at day 11 (Fig. 3F).

To determine which stage of myeloid differentiation is affected by NYT, we carried out CFU assays. No colonies were produced without addition of cytokines (T. Inoue, K. Kulkeaw and K. Muennu, unpublished data). In the presence of the myeloid cytokines SCF, IL-3, and IL-6, NYT increased total colony number 1.30-fold ($P = 0.528$). Among those colonies, the number of CFU-M, CFU-G, and CFU-GM, all indicative of committed myeloid progenitors, increased, implying that NYT accelerates myelopoiesis at the progenitor level (Fig. S4 in Supporting information).

Gene expression changes in bone marrow cells

To identify hematopoietic genes regulated by NYT, microarray analysis was carried out to compare BM MNCs cultured with and without NYT for 11 days. Up-regulated ($P < 0.05$) and down-regulated ($P < 0.05$) genes were analyzed and categorized functionally (Fig. S5 in Supporting information). In agreement with results shown in Fig. 3F and Fig. S4, we identified factors affecting leukopoiesis. Among them, we observed down-regulation of *Rasgrp1* (de la Luz Sierra *et al.* 2010) and *Dok2* (Garcia *et al.* 2004) after 11 days in culture with NYT (7.31-fold decrease ($P = 0.0005$) and 1.78-fold decrease ($P = 0.003$), respectively) (Fig. 3G), a finding validated by real-time PCR.

Discussion

Here, we assessed molecular mechanisms underlying the effect of Kampo medicines on erythropoiesis. Among four such medicines tested, NYT showed the greatest stimulation of BM MNC proliferation accompanied by the highest up-regulation of *Myc*, a factor associated with up-regulated proliferation, by 11 days after culture (Fig 1B). Relevant to proliferation, our findings are in accordance with a report that NYT increased the number of primary rat oligodendrocyte precursors *in vitro* as assessed by BrdU incorporation studies (Kobayashi *et al.* 2003).

Previously, others had shown that after induction of anemia, NYT stimulates erythroid cell differentiation (Takatsuki *et al.* 1996; Takano *et al.* 2009). Thus, we initially hypothesized that Kampo medicines would accelerate erythropoiesis. However, in our cul-

Figure 3 Effect of NYT on myeloid differentiation of BM $CD45^+$ cells. (A) $CD45^+/Ter119^-$ leukocytes were isolated from BM MNCs to remove erythroid cells and cultured for 11 days. (B) Viable cells were collected at days 4, 8, and 11 and counted using trypan blue dye. (C) BM $CD45^+$ leukocytes cultured with and without NYT were collected at day 11, and leukocyte differentiation was assessed by flow cytometry based on CD45 staining. The percentage of $CD45^+$ leukocytes is shown at right. (D) Myeloid differentiation of $CD45^+$ cells was evaluated by flow cytometry at day 11 based on staining with Mac-1 (CD11b) and F4/80. The percentage of $CD45^+/Mac\text{-}1^+/F4/80^+$ macrophages is shown at right. (E) Granulocyte differentiation of $CD45^+$ cells was evaluated by flow cytometry at day 11 based on staining with Mac-1 (CD11b) and Gr-1. The percentage of $CD45^+/Mac\text{-}1^+/Gr\text{-}1^+$ granulocytes is shown at right. (F) Quantitative real-time PCR analysis of expression of the myeloid genes *Pu.1* and *Csf1r* at days 4, 8, and 11. Data were assessed by normalized values to control at day 4. (G) BM MNCs cultured with and without NYT *in vitro* were collected and analyzed by quantitative real-time PCR at day 11 for expression of *Rasgrp1*, a lymphopoietic gene, and *Dok2*, a myelopoietic gene. Data are normalized to β-*actin* expression.

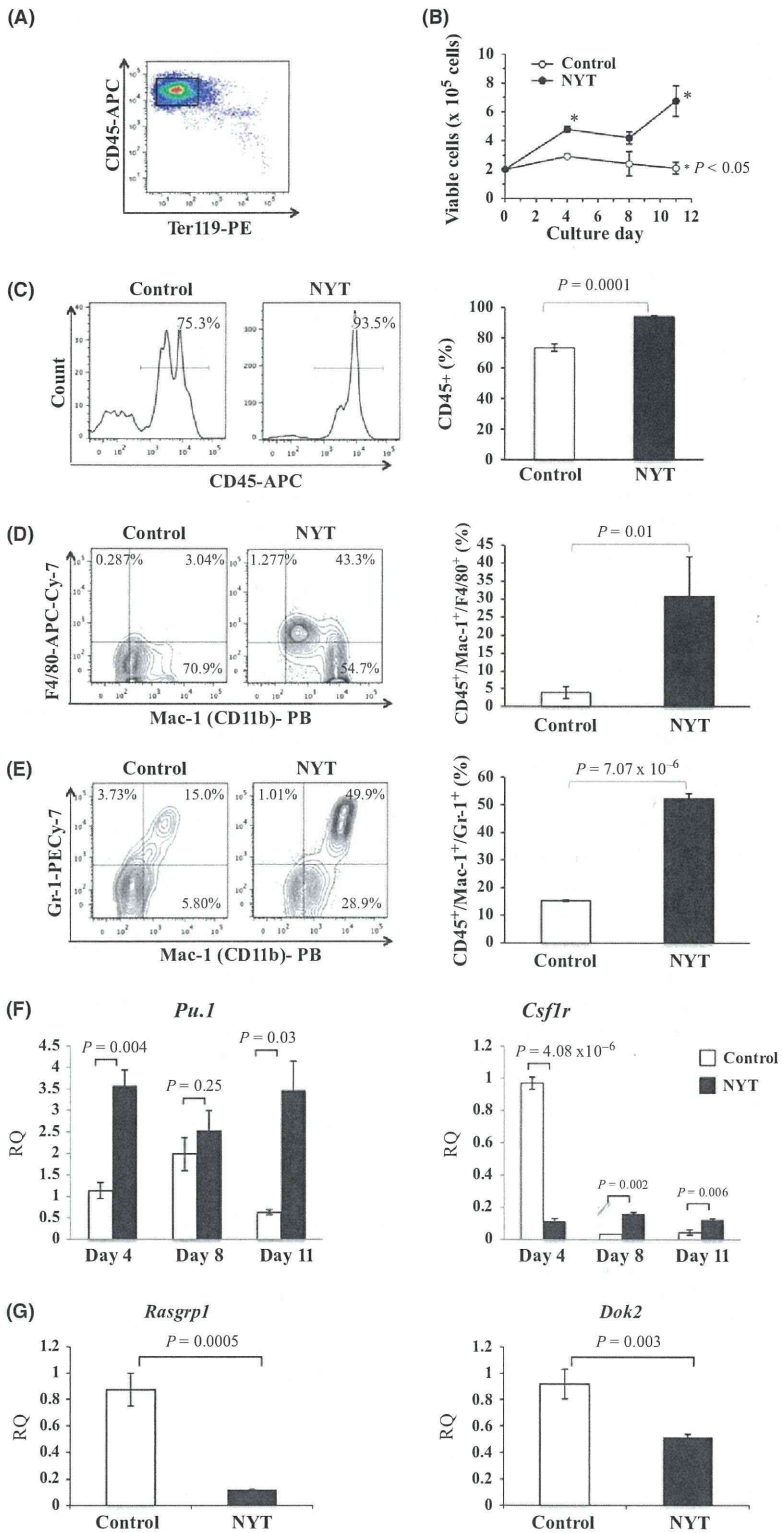

ture conditions, we did not observe up-regulation of *Gata1* and *Klf1* mRNAs or of Ter119 proteins—markers of erythropoiesis—after NYT treatment (Fig. S3 in Supporting information). These discrepancies suggest that NYT activity may differ in normal homeostasis compared with anemic conditions. However, when we evaluated leukopoiesis, we found that culturing BM MNCs for 11 days in NYT accelerated myelopoiesis but not lymphopoiesis, based on flow cytometric and gene expression analysis (Fig. S3B in Supporting information). Previously, Okamura *et al.* reported that NYT dose dependently augmented production of GM-CSF but not G-CSF, as evaluated by ELISA analysis of human peripheral blood MNCs after 3 days of culture (Okamura *et al.* 1991). However, we did not observe expression of *GM-CSF* and *G-CSF* transcripts at days 4, 8, or 11 in $CD45^+$ cells derived from BM MNCs cultured with NYT (T. Inoue, K. Kulkeaw and K. Muennu, unpublished data). These discrepancies may be attributable to species differences or culture conditions. Miura *et al.* reported that intraperitoneal NYT administration in mice increased the number of macrophages in both the peritoneal cavity and spleen within 7 to 10 days (Miura *et al.* 1989).

Some bioactive ingredients of JTT, such as polysaccharides and fatty acids, reportedly have proliferative effect on hematopoietic cells. Polysaccharides obtained from Glycyrrhiza, a component of JTT exhibited mitogenic activity that influences the selective proliferation of B cells (Yamada & Saiki 2005). Fatty acids, such as oleic and linoleic acids, stimulate the proliferation of hematopoietic stem cells *in vitro* (Hisha *et al.* 1997). As Kampo medicines tested in this study originally include polysaccharides and fatty acids, we cannot deny the possibility that these bioactive ingredients of NYT might affect the myeloid cell proliferation from BM MNCs (Fig. 1B). It will be a topic in the future.

In summary, we provide the molecular evidence that NYT accelerates myelopoiesis *in vitro*.

Experimental procedures

Mice

C57BL/6 (2–4 months) mice were purchased from Nihon SLC (Hamamatsu, Japan) and Kyudo (Tosu, Japan). Animals were handled according to the Guidelines for Laboratory Animals of Kyushu University. This study was approved by the Animal Care and Use Committee, Kyushu University (Approval ID: A21-068-0).

Preparation of Kampo medicines

Kampo medicines including NYT, SMT, JTT, and DBT (Table S1 and Fig. S1 in Supporting information) (Tsumura & Co, Tokyo, Japan) were freshly prepared as follows. First, 0.25 g of each Kampo medicine extract powder was dissolved in 5 mL of hot distilled water (at a final concentration of 50 mg/mL). The solution was centrifuged at 2395 ***g*** for 10 min, and supernatants were filtered through 0.45-μm filters.

Primary cell culture

BM cells were harvested by flushing femurs of 2–4 months C57BL/6 mice with Iscove's Modified Dulbecco's Medium (IMDM, SIGMA-ALDRICH, St. Louis, MO) supplemented with 2% fetal bovine serum (FBS). After one PBS wash, cells were incubated with red blood cell lysis buffer (0.16 M NH_3Cl, 10 mM $KHCO_3$, 5 mM EDTA) on ice for 10 min, and then mononuclear cells (MNCs) were separated using Lympholyte-M (Density: 1.0875 + 0.0010 g/cm^3, CEDARLANE®) according to the manufacturer's instruction. BM MNCs were cultured with IMDM containing 10 μg/mL Kampo supernatant, 15% FBS, 0.1% 2-mercaptoethanol, and 10 U/mL penicillin/10 μg/mL streptomycin (SIGMA-ALDRICH). Negative controls were cultured in the same media without Kampo medicines. Cells were incubated at 37 °C, 5% CO_2, and 95% humidity. Culture media were changed at day 8. Cells were collected for counting and analysis at days 4, 8, and 11 of culture. The number of viable cells was determined using trypan blue staining. To assess the effect of Kampo medicines on $CD45^+$ leukocytes, BM MNCs were stained with anti-CD45-APC antibody (Ab) (eBioscience, San Diego, CA) and sorted using a FACS Aria cell sorter (BDIS, San Jose, CA). $CD45^+$ cells were cultured with respective Kampo medicines and noncytokine-containing medium according to methods described above.

Quantitative real-time PCR

Total RNA was extracted from cultures of BM MNCs and $CD45^+$ cells using a RiboPure™ Kit (Life Technologies, Carlsbad, CA). Total RNA was subjected to reverse transcription using a High-Capacity RNA-to-cDNA Kit (Life Technologies) according to established protocols. Gene expression levels were measured by StepOnePlus™ Real-Time PCR (Life Technologies) with TaqMan® Gene Expression Master Mix. All probes (*Myc, Gata1, Pu.1, Csf1r, Rasgrp1* and *Dok2*) were from TaqMan® Gene Expression Assays. PCR conditions were as follows: denaturation at 95 °C for 10 s, annealing at 60 °C for 20 s (40 cycles), and extension at 72 °C for 20 s. A final dissociation stage was carried out consisting of 95 °C for 15 s, 60 °C for 1 min, and 95 °C for 15 s. β-*actin* served as internal control. Normalized values ($-2^{\Delta\Delta C_T}$, ddCT) were compared among samples, and experiments were carried out in triplicate.

Microarray analysis

BM MNCs cultured with NYT or negative controls were collected at day 11. Total RNA was extracted using RNeasy® Plus Micro Kit (QIAGEN). RNA concentration was measured by NANODROP 2000c (Thermo Fisher Scientific). cRNA was amplified, labeled, and hybridized to an Agilent Whole Mouse GE 4 × 44K v2 Microarray (Agilent Technologies, Santa Clara, CA, USA) according to the manufacturer's instructions. All hybridized microarrays were scanned using an Agilent scanner, and signals of all probes were analyzed using Feature Extraction Software (9.5.1.1) (Agilent Technologies).

Flow cytometry

To analyze erythroid differentiation, cells were stained with anti-Ter119-PE Ab and anti-CD71-FITC Ab (BD Bioscience). To analyze myeloid and lymphoid differentiation, cells were stained with anti-Mac-1-PB Ab (Biolegend, San Diego, CA) and anti-B220-APC-Cy7 Ab (Biolegend). To isolate $CD45^+Ter119^-$ cells, BM MNCs were stained with anti-CD45-APC Ab (Biolegend) and anti-Ter119-PE Ab. To identify leukocytes, $CD45^+$ cultured cells were stained with anti-Mac-1-PB Ab, anti-F4/80-APC-Cy7 Ab (Biolegend) and anti-Gr-1-PE-Cy7 Ab (Biolegend).

Colony formation assay

BM MNCs were suspended in 4 mL of MethoCult® GF M3234 (Stemcell Technologies) supplemented with IL-3 (10 ng/mL), IL-6 (10 ng/mL), and SCF (50 ng/mL) and distributed into three 35-mm dishes (1×10^4 cells/dish). Cells were then incubated with 5% CO_2 at 37 °C. Colonies were counted on days 10–12 using an inverted phase-contrast microscope CKX41 (Olympus, Tokyo, Japan).

Statistical analysis

Data are presented as means plus standard deviation (SD). Student's *t*-test was used to calculate statistical significance. A *P*-value <0.05 was considered statistically significance.

Acknowledgements

This work was supported by a grant from the Ministry of Health, Labour and Walfare, Japan and by a bilateral program between Japan and Thailand, which are supported by the Japan Society for the Promotion of Science (JSPS) and National Research Council of Thailand (NRCT). T. Inoue and K. Kulkeaw were supported by postdoctoral fellowships for Young Scientists from the JSPS. K. Muennu was supported by a postdoctoral fellowship from Mahidol University, the Heiwa Nakajima Foundation and Prince of Songkla University. The authors would like to thank Drs. F. Suthat, S. Saovaros, K. Akashi for helpful discussion, and Dr. Elise Lamar for critical reading of the manuscript.

References

Ando, N. (1999) Blood making effect of Ninjin-yoei-to (Ren-shen-yang-rong-tang) as monotherapy in obesteric and gynecologic patient with anemia. *Jpn. J. Orient. Med.* **50**, 461–470.

Garcia, A., Prabhakar, S., Hughan, S., Anderson, T.W., Brock, C.J., Pearce, A.C., Dwek, R.A., Watson, S.P., Hebestreit, H.F. & Zitzmann, N. (2004) Differential proteome analysis of TRAP-activated platelets: involvement of DOK-2 and phosphorylation of RGS proteins. *Blood* **103**, 2088–2095.

Hisha, H., Yamada, H., Sakurai, M.H., Kiyohara, H., Li, Y., Yu, C., Takemoto, N., Kawamura, H., Yamamura, K., Shinohara, S., Komatsu, Y., Aburada, M. & Ikehara, S. (1997) Isolation and identification of hematopoietic stem cell-stimulating substances from Kampo (Japanese herbal) medicine, Juzen-taiho-to. *Blood* **90**, 1022–1030.

Kobayashi, J., Seiwa, C., Sakai, T., Gotoh, M., Komatsu, Y., Yamamoto, M., Fukutake, M., Matsuno, K., Sakurai, Y., Kawano, Y. & Asou, H. (2003) Effect of a traditional Chinese herbal medicine, Ren-Shen-Yang-Rong-Tang (Japanese name: Ninjin-Youei-To), on oligodendrocyte precursor cells from aged-rat brain. *Int. Immunopharmacol.* **3**, 1027–1039.

de la Luz Sierra, M., Sakakibara, S., Gasperini, P., Salvucci, O., Jiang, K., McCormick, P.J., Segarra, M., Stone, J., Maric, D., Zhu, J., Qian, X., Lowy, D.R. & Tosato, G. (2010) The transcription factor Gfi1 regulates G-CSF signaling and neutrophil development through the Ras activator RasGRP1. *Blood* **115**, 3970–3979.

McGrath, K. & Palis, J. (2008) Ontogeny of erythropoiesis in the mammalian embryo. *Curr. Top. Dev. Biol.* **82**, 1–22.

Miller, I.J. & Bieker, J.J. (1993) A novel, erythroid cell-specific murine transcription factor that binds to the CACCC element and is related to the Kruppel family of nuclear proteins. *Mol. Cell. Biol.* **13**, 2776–2786.

Miura, S., Kawamura, I., Yamada, A., Kawakita, T., Kumazawa, Y., Himeno, K. & Nomoto, K. (1989) Effect of a traditional Chinese herbal medicine ren-shen-yang-rong-tang (Japanese name: ninjin-youei-to) on hematopoietic stem cells in mice. *Int. J. Immunopharmacol.* **11**, 771–780.

Miyazaki, T., Uchini, H., Kimura, I., Saito, H., Shibaa, A., Takaku, F., Niho, Y., Matsuda, T., Miura, A., Imamura, M., Kitamura, K. & Hotta, T. (1994) Effects of Ren-shen-yang-rong-tang (Japanese name: Ninjin-youei-to), a traditional herbal medicine, on the hematopoiesis in the patients with aplastic anemia. *Rinsyou Iyaku* **10**, 189–201.

Motoo, Y., Mouri, H., Ohtsubo, K., Yamaguchi, Y., Watanabe, H. & Sawabu, N. (2005) Herbal medicine Ninjinyoeito ameliorates ribavirin-induced anemia in chronic hepatitis C: a randomized controlled trial. *World J. Gastroenterol.* **11**, 4013–4017.

Nagoshi, H., Irako, A., Takahashi, A., Fukumura, R., Nomura, M., Takahashi, S., Isobe, H., Ide, K. & Someya, K. (1993) Clinical effect of Ren-Shen-Yang-Rong-Tang (Japanese

Name: Ninjin-Yoei-To) on refractory anemia in the Elderly. *Jpn Pharmacol. Ther.* **21**, 4789–4795.

Ohmori, M., Suzuki, T., Omori, S. & Yasuda, N. (1993) A case of aplastic anemia-PNH syndrome treated with a traditional chinese herbal medicine, EK-108. *Jpn Pharmacol. Ther.* **21**, 553–556.

Ohmori, S., Usui, T., Yasuda, N., Ohmori, M., Yamagishi, M. & Okuma, M. (1992) Improvement of anemia by administration of EK-108 [Chinese herbal medicine, Ren-Shen-Yang-Rong-Tang (Japanese name, Ninjin-Yoei-To)] in a patient of myelodisplastic syndrome. *Jpn Pharmacol. Ther.* **20**, 361–365.

Okamura, S., Shimoda, K., Yu, L.X., Omori, F. & Niho, Y. (1991) A traditional Chinese herbal medicine, ren-shen-yang-rong-tang (Japanese name: ninjin-yoei-to) augments the production of granulocyte-macrophage colony-stimulating factor from human peripheral blood mononuclear cells in vitro. *Int. J. Immunopharmacol.* **13**, 595–598.

Takano, F., Ohta, Y., Tanaka, T., Sasaki, K., Kobayashi, K., Takahashi, T., Yahagi, N., Yoshizaki, F., Fushiya, S. & Ohta, T. (2009) Oral Administration of Ren-Shen-Yang-Rong-Tang 'Ninjin'yoeito' Protects Against Hematotoxicity and Induces Immature Erythroid Progenitor Cells in 5-Fluorouracil-induced Anemia. *Evid. Based Complement. Alternat. Med.* **6**, 247–256.

Takatsuki, F., Miyasaka, Y., Kikuchi, T., Suzuki, M. & Hamuro, J. (1996) Improvement of erythroid toxicity by lentinan and erythropoietin in mice treated with chemotherapeutic agents. *Exp. Hematol.* **24**, 416–422.

Takemura, K. (2000) Effect of Ninjin-Youeitoh on renal anemia in hemodialysis patients treated by recombinant human erythropoietin. *Kampo to Saishintiryou* **9**, 271–274.

Whitelaw, E., Tsai, S.F., Hogben, P. & Orkin, S.H. (1990) Regulated expression of globin chains and the erythroid transcription factor GATA-1 during erythropoiesis in the developing mouse. *Mol. Cell. Biol.* **10**, 6596–6606.

Yamada, H. & Saiki, I. (2005) *Juzen-taiho-to (Shi-Quan-Da-Bu-Tang): Scientific Evaluation and Clinical Applications*. Boca Raton, FL: CRC Press.

Yanagihori, A., Miyagi, M., Hori, M., Ohtaka, K., Matsushima, H. & Itoh, M. (1995) Effect of Ninjin-Yoei-To on iron-deficiency anemia. *Rinsyou to Kenkyu* **72**, 231–234.

Received: 18 November 2013
Accepted: 29 January 2014

Supporting Information

Additional Supporting Information may be found in the online version of this article at the publisher's web site:

Figure S1 3D HPLC pattern of Kampo medicines.

Figure S2 Hematopoietic cell proliferation in the presence of NYT and its components.

Figure S3 Effect of NYT on leukopoiesis of BM MNCs.

Figure S4 NYT accelerates hematopoietic colony formation.

Figure S5 Global changes in gene expression observed in NYT-treated BM cells.

Table S1 Components of four Kampo medicines

Cancer Science
Japanese Cancer Association JCA
Open Access

Characterization of common marmoset dysgerminoma-like tumor induced by the lentiviral expression of reprogramming factors

Saori Yamaguchi,[1,9] Tomotoshi Marumoto,[1,2,9] Takenobu Nii,[1] Hirotaka Kawano,[1] Jiyuan Liao,[1] Yoko Nagai,[1] Michiyo Okada,[1] Atsushi Takahashi,[3] Hiroyuki Inoue,[1,2] Erika Sasaki,[4] Hiroshi Fujii,[5] Shinji Okano,[5] Hayao Ebise,[6] Tetsuya Sato,[7] Mikita Suyama,[7] Hideyuki Okano,[8] Yoshie Miura[1] and Kenzaburo Tani[1,2]

[1]Division of Molecular and Clinical Genetics, Molecular and Clinical Genetics, Medical Institute of Bioregulation, Kyushu University, Fukuoka; [2]Department of Advanced Molecular and Cell Therapy, Kyushu University Hospital, Fukuoka; [3]Division of Translational Cancer Research Medical Institute of Bioregulation, Kyushu University, Fukuoka; [4]KEIO-RIKEN Research Center for Human Cognition, Keio University, Tokyo; [5]Division of Pathophysiological and Experimental Pathology, Department of Pathology, Kyushu University, Fukuoka; [6]Genomic Science Laboratories, Dainippon Sumitomo Pharma, Osaka; [7]Division of Bioinformatics, Medical Institute of Bioregulation, Kyushu University, Fukuoka; [8]Department of Physiology, Keio University, Tokyo, Japan

Key words

Common marmoset, FGFR, regenerating medicine, reprogramming factor, tumorigenesis

Correspondence

Kenzaburo Tani, Division of Molecular and Clinical Genetics, Department of Molecular Genetics, Medical Institute of Bioregulation, Kyushu University, 3-1-1 Maidashi, Higashi-ku, Fukuoka 812-8582 Japan.
Tel: +81-92-642-6434; Fax: +81-92-642-6444;
E-mail: taniken@bioreg.kyushu-u.ac.jp

[9]These authors contributed equally to this work.

Funding information

Project for Realization of Regenerative Medicine (08008010) and Kakenhi (23590465) from the Ministry of Education, Culture, Sports, Science and Technology (MEXT), Japan.

Received June 4, 2013; Revised January 14, 2014; Accepted February 5, 2014

Cancer Sci **105** (2014) 402–408

doi: 10.1111/cas.12367

Recent generation of induced pluripotent stem (iPSCs) has made a significant impact on the field of human regenerative medicine. Prior to the clinical application of iPSCs, testing of their safety and usefulness must be carried out using reliable animal models of various diseases. In order to generate iPSCs from common marmoset (CM; *Callithrix jacchus*), one of the most useful experimental animals, we have lentivirally transduced reprogramming factors, including POU5F1 (also known as OCT3/4), SOX2, KLF4, and c-MYC into CM fibroblasts. The cells formed round colonies expressing embryonic stem cell markers, however, they showed an abnormal karyotype denoted as 46, X, del(4q), +mar, and formed human dysgerminoma-like tumors in SCID mice, indicating that the transduction of reprogramming factors caused unexpected tumorigenesis of CM cells. Moreover, CM dysgerminoma-like tumors were highly sensitive to DNA-damaging agents, irradiation, and fibroblast growth factor receptor inhibitor, and their growth was dependent on c-MYC expression. These results indicate that DNA-damaging agents, irradiation, fibroblast growth factor receptor inhibitor, and c-MYC-targeted therapies might represent effective treatment strategies for unexpected tumors in patients receiving iPSC-based therapy.

The development of a technology to generate iPSCs from differentiated somatic cells by the transduction of a set of transcription factors, OSKM, made a significant impact in the field of basic research for regenerative medicine, in light of their potential use as a cell source for transplantation therapy for various kinds of incurable diseases.[1,2]

However, the low efficiency of iPSC generation, the need to induce their efficient differentiation into specific cell types, and the risk of tumor formation in recipients transplanted with iPSC-derived functional cells have hindered the clinical application of iPSCs.[3] The transduction of transcription factors, including the oncogene *c-MYC*, insertional mutation of the genome caused by virus vectors, and genomic instability due to the stress of long-term culture for reprogramming, might contribute to tumor development when iPSC-derived functional cells are applied to clinical practice.[4] Although the technology used to generate iPSCs has improved with the use of OSK without M,[5] non-viral vectors,[6] other molecules such as mRNA or miRNA,[7] and chemicals,[8] tumor formation in recipients remains a major concern.[9] Despite these issues, reprogramming factor-related tumor cells have not been well-characterized to date.

The CM (*Callithrix jacchus*) has several advantages as an experimental laboratory primate, including ease of handling, being inexpensive to house and feed, and a high reproductive rate.[10] Therefore, CM and CM-derived iPSCs represent useful experimental tools for testing the clinical utility of iPSC-based regenerative medicine *in vivo* and *in vitro*.

In this study, we attempted to generate iPSCs from CM fibroblasts, and inadvertently produced immature malignant tumor cells. We therefore analyzed the biological characteristics of these cells *in vitro* and *in vivo*. The results may provide useful information for the development of strategies to deal with tumors unexpectedly formed in patients treated with iPSC-based therapies.

Materials and Methods

Cell culture, induction of reprogramming, and proliferation assay. Common marmoset ARCs, CM ESCs, and iPS A cells derived from fetal liver cells (provided by Erika Sasaki, KEIO-REKEN Research Center for Human Cognition, Keio University, Tokyo, Japan) were maintained in DMEM/F12 (Sigma-Aldrich, St. Louis, MO, USA) containing 20% Knockout Serum Replacement (Gibco, Carlsbad, CA, USA), 0.1 mM non-essential amino acid (Gibco), 1 mM L-glutamine (Nacalai Tesque, Kyoto, Japan), 1% antibiotic–antimycotics (Nacalai Tesque), 0.4 mM 2-mercaptoethanol (Sigma Aldrich), and 0.12% sodium hydroxide (Nacalai Tesque). The CM DGs were maintained in DMEM/F12 containing 10% FBS at 37°C in a 5% humidified CO_2 atmosphere. Detailed descriptions of the cell culture, reprogramming method, and proliferation assay are provided in Figures 1 and 5.

Plasmids and lentiviral vector production. Human OCT3/4, SOX2, KLF4, or c-MYC was inserted into CSIV-CMV-MCS-IRES2-Venus lentiviral vectors (kindly provided by Hiroyuki Miyoshi, Riken, Tsukuba, Japan). Short hairpin RNAs targeting OCT3/4, SOX2, and c-MYC were obtained from Addgene (Cambridge, MA, USA), and shRNA targeting KLF4 was obtained from Applied Biological Materials (Richmond, BC, Canada). Lentiviruses were produced as previously described.[11]

Microarray analysis. Total RNA from AGM fibroblasts, ARCs, and iPS A cells were isolated using the RNeasy Mini Kit (Qiagen, Valencia, CA, USA). RNA was reverse-transcribed, biotin-labeled, and hybridized for 16 h to a marmoset genome oligonucleotide custom array Marmo2 (in preparation),[12] which was subsequently washed and stained in a Fluidics Station 450 (Affymetrix, Santa Clara, CA, USA) according to the manufacturer's instructions. Detailed protocols of microarray analysis are provided in Figures 2 and S5.

DNA-damaging treatments. The CM DGs were treated with 1 μg/mL MMC (Kyowa Hakko Kirin, Tokyo, Japan) or 10 μg /mL cisplatin (Sigma-Aldrich) for 1 h at 37°C. For irradiation, CM DGs were irradiated (20 Gy) using Gammacell 40 (Atomic Energy, Chalk River, Ontario, Canada). At 24 h after treatment, the cells were stained with propidium iodide (Nacalai Tesque), and the proportion of dead cells was analyzed as the sub-G_1 population by flow cytometry (FACSCalibur; BD Biosciences, San Jose, CA, USA).

Statistical analysis. Statistical analyses were carried out with the GraphPad Prism 5.0d software package (GraphPad Software, La Jolla, CA, USA). Statistical analyses were carried out using a two-tailed unpaired Student's *t*-test or one-way ANOVA followed by Tukey's multiple comparison test. $P < 0.05$ was considered statistically significant.

Additional information is provided in Supporting information.

Results

Characteristic of aorta-gonado-mesonephros fibroblast-derived colonies formed by transduction of reprogramming factors. To generate CM-derived iPSCs, reprogramming factors (OSKM) were transduced into AGM fibroblasts using lentiviral vectors (Fig. 1a). Then OSKM-transduced cells were transferred to mouse embryonic fibroblast feeder cells on day 7 post-infection, and cultured in medium for CM ESCs. We found that the cells formed sphere-like structures on day 17 post-infection (Fig. 1b). Moreover, these colonies showed AP activity

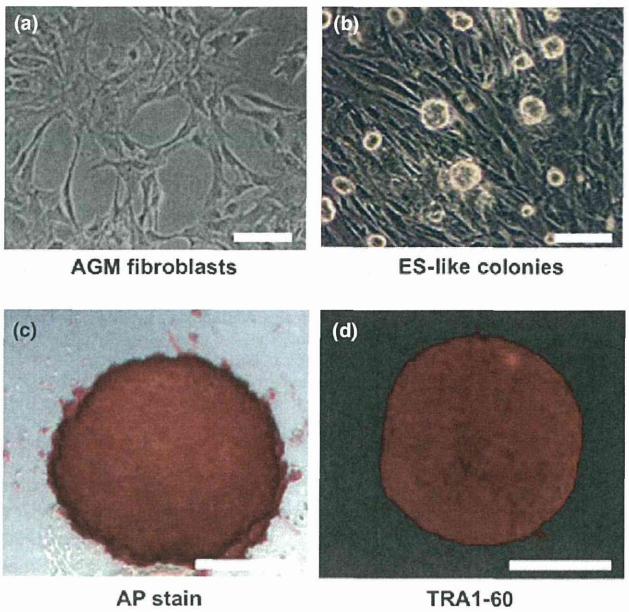

Fig. 1. Characterization of aorta-gonado-mesonephros (AGM) fibroblast-derived colonies formed by transduction of reprogramming factors. Representative phase-contrast images of (a) AGM fibroblasts and (b) abnormally reprogrammed cells (ARCs) forming round-shaped colonies. (c) Representative image showing expression of alkaline phosphatase (AP) activity in ARCs. (d) Immunocytochemical staining showing expression of TRA1-60 in ARCs. Bar = 100 μm.

(Fig. 1c), and expressed ESC markers such as TRA1-60, SALL1, LIN28, and DPPA4 (Figs 1d, S1). These results suggested that the reprogrammed AGM fibroblasts formed immature, round iPSC-like colonies.

Chromosome abnormality and tumor-forming ability in abnormally reprogrammed cells. Given that *KLF4* and *c-MYC* are well-known oncogenes,[13,14] transduction with OSKM transcription factors may cause cell transformation and chromosome instability.[15] We carried out karyotype analysis of the colony-forming cells to determine if OSKM-transduced AGM fibroblasts exhibited chromosome instability. The normal karyotype of CM cells is 44 autosomes and two sex chromosomes (46, XX or 46, XY).[16] However, the round colony-forming cells contained 44 autosomes, one X chromosome, and an abnormal marker chromosome (mar), with deletions of chromosome 4q, and were therefore denoted as 46, X, del (4q), +mar (Fig. 2a, right panel). The karyotype of the parental AGM fibroblasts was 46, X, +mar (Fig. 2a, left panel). These results suggested that the reprogramming stress induced by OSKM might have caused the deletion of 4q, although the possibility that the stress of long-term *in vitro* culture might have resulted in chromosome instability could not be excluded. These colony-forming cells were named ARCs.

To examine the ability of ARCs to differentiate into three germ layers like ESCs, we carried out an *in vitro* differentiation assay based on the protocol for human ESC differentiation.[17,18] Unlike human ESCs, ARCs did not differentiate into neural progenitors, cardiomyocytes, or hepatic cells (Fig. S2, Video S1).

We carried out *in vivo* differentiation assays by injecting ARCs into the testes of SCID mice. Approximately 6 weeks after injection, 11 of 18 mice injected with ARCs showed

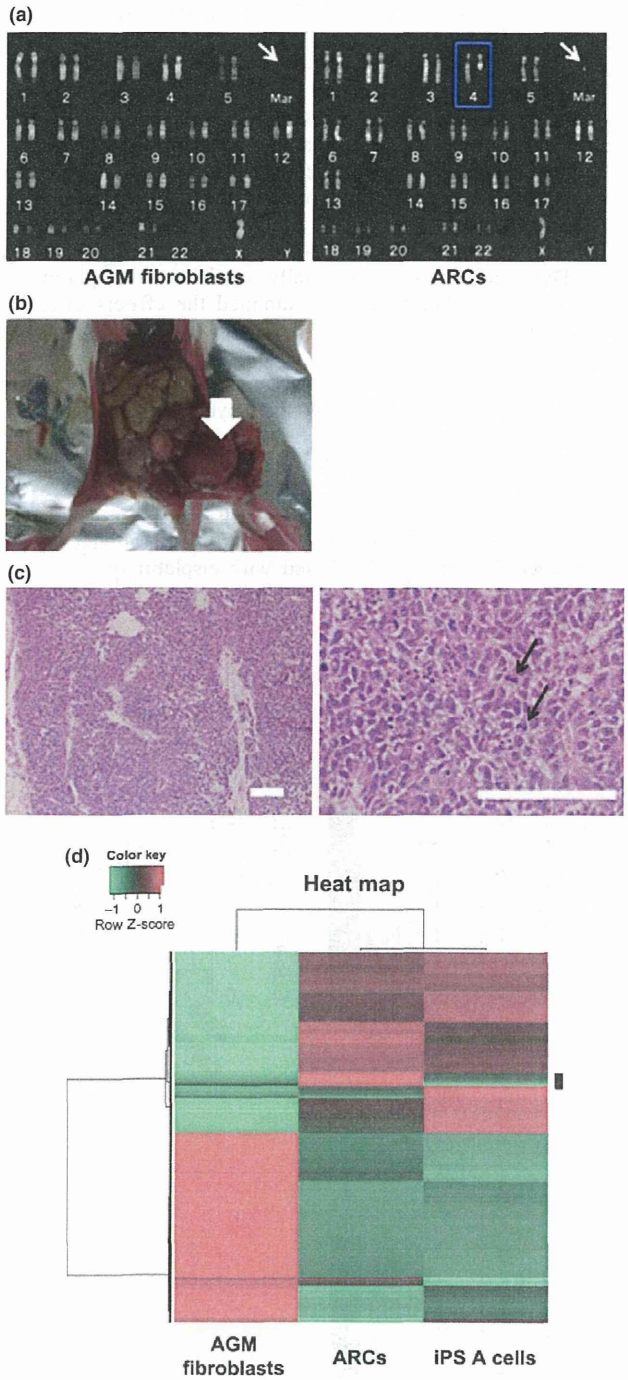

Fig. 2. Chromosome abnormality and tumor-forming ability in abnormally reprogrammed cells (ARCs). (a) Karyotype analyses of aorta-gonado-mesonephros (AGM) fibroblasts (left panel) and ARCs (right panel). Arrows indicate marker chromosome. Blue outline indicates the deletion of 4q. Mar, marker chromosome. (b) Representative photograph of dysgerminoma-like tumor (arrow) formed by transplantation of ARCs into SCID mice. (c) Hematoxylin-eosin staining of dysgerminoma-like tumor tissues. Arrows in right panel indicate mitotic figures in tumor cells. Bar = 100 μm. (d) Microarray analysis. Gene expressions in AGM fibroblasts, ARCs, and normal induced pluripotent stem (iPS) A cells were analyzed by unsupervised hierarchical clustering. A heat map using probes showing differential expression levels in each cell line is shown. Red indicates upregulation; green indicates downregulation. The black bar on the right side of the heat map shows candidate differentially expressed probes in ARCs.

tumor formation (Fig. 2b), whereas no mice injected with AGM fibroblasts showed tumor formation (0/3, data not shown). Staining with H&E revealed that the tumors were relatively homogenous, with high cellular density, necrosis, and pleomorphism, indicating their malignant phenotype (Fig. 2c). In addition, tumors were composed of nests and sheets of uniform round or polygonal cells with abundant, clear to faintly eosinophilic cytoplasm with well-demarcated cytoplasmic borders and a delicate network of thin-walled blood vessels in the tumor nests (Fig. 2c, right panel). Furthermore, immunohistochemical analyses revealed that the tumor cells were focally and weakly immunopositive for vimentin, and immunonegative for the differentiation markers cytokeratin, S100, desmin, α-smooth muscle actin, and neuron-specific enolase (data not shown). Tumor tissues also expressed c-KIT, but not CD30 or CD45 (Fig. S3). These molecular expression profiles implied that the tumor was equivalent to human malignant dysgerminoma, rather than other types of immature tumors such as embryonal carcinoma, yolk sac tumor, or teratoma.[19,20] The tumor was named CM DG.

We next carried out soft agar assays to determine if ARCs were transformed and showed anchorage-independent growth as a result of ectopic expression of reprogramming factors. The ARCs were cultured in 0.5% agarose-containing medium for 20 days, and the number of colonies was counted. The ARCs formed many colonies, compared with parental AGM fibroblasts (Fig. S4a and data not shown). These results strongly suggested that ARCs were transformed during reprogramming, and acquired the capacity for anchorage-independent growth. To clarify the contribution of reprogramming factors that could transform AGM fibroblasts, we transduced various combinations of these factors into AGM fibroblasts, and examined if the transduced cells were transformed by the colony formation assay on mouse embryonic fibroblasts, AP staining assay, and soft agar assay. The iPSC-like colonies were found in OSKM- and OSM-transduced cells (OSKM, 30 ± 3/5000; OSM, 6 ± 0/5000), but they were not found at all when OSK, OS, OM, SM, O, S, K, or M were transduced (Fig. S4b). AP activity was found in both OSKM- and OSM-transduced cells, although OSM-transduced cells showed weaker AP activity than OSKM-transduced cells (Fig. S4c). In soft agar assay, the anchorage-independent growth was found in both OSKM- and OSM-transduced cells (Fig. S4d; OSKM, 160 ± 23/1000; OSM, 163 ± 10/1000). These results indicated that the simultaneous expression of OCT3/4, SOX2, and c-MYC was at least required for the transformation of AGM fibroblasts, while KLF4 did not play a major role in the transformation of AGM fibroblasts.

Tomioka *et al.* reported the establishment of CM iPSCs (iPS A cells) showing normal karyotype.[12] To characterize the gene expression in ARCs, we carried out microarray analyses using mRNA from ARCs, iPS A cells, and AGM fibroblasts. According to the clustering pattern and the heat map, 171 probes that showed higher expression levels in ARCs as compared to other cells were selected as candidate differentially expressed genes in ARCs (Fig. 2d). Moreover, we focused on the genes specifically highly expressed in ARCs compared to those in iPS A cells, and the top seven genes highly expressed in ARCs were selected (*ZFHX4*, *PCDH19*, *NFIX*, *HOXC8*, *STMN2*, *SERPINA3*, and *CXORF67*). Then we validated these data by semiquantitative RT-PCR analyses, and five genes (*ZFHX4*, *NFIX*, *HOXC8*, *STMN2*, and *CXORF67*) were confirmed to be more expressed in ARCs than those in controls (Fig. S5). The high expression of these five genes might be characteristics of ARCs.

Characteristic of CM DGs. We then surgically removed CM DGs and cultured them *in vitro* to examine their biological characteristics. The CM DGs could grow infinitely in a semi-floating state in the culture dish, and showed continuous expression of Venus fluorescent protein (Fig. 3a,b). We generated five CM DG cell lines (CMY401, CMY402a, CMY402b, CMY403a, and CMY403b) from five independent tumors formed by the injection of ARCs into SCID mice, and found that all four transduced reprogramming factors were integrated into their genomes (Fig. S6a). Both endogenous and exogenous reprogramming factors were expressed in these cell lines (Fig. 3c,d).

Effects of DNA-damaging agents and irradiation on CM DGs. Dysgerminomas are generally sensitive to cisplatin and irradiation.[21,22] We therefore examined the effects of DNA-damaging agents such as MMC and cisplatin on CM DGs. Three CM DG cell lines (CMY402a, CMY402b, and CMY403a) were treated with MMC for 1 h, and the proportion of dead cells was analyzed by flow cytometry at 24 h after treatment. The percentage of cells with a sub-G_1 DNA content was taken as a measure of dead cells in the population. The proportion of dead cells in MMC-treated CM DG cultures was significantly higher than that in controls (MMC-treated AGM fibroblasts) (Figs 4a, S7). Similar results were obtained when these three cell lines were treated with cisplatin or irradiation (Figs 4b,c, S8, S9). These results suggested that CM DGs were

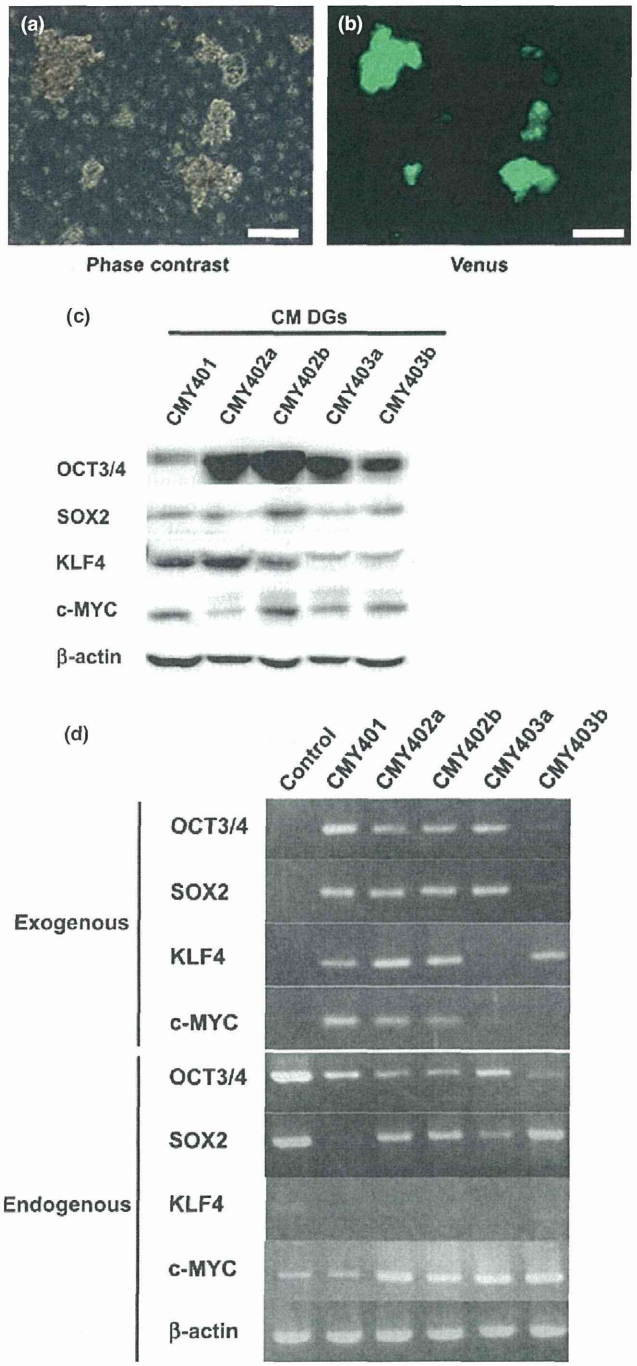

Fig. 3. Characterization of common marmoset dysgerminoma-like (CM DG) cells in culture. (a) Representative phase-contrast image of CM DGs. (b) Immunofluorescent image of Venus expression in CM DGs. Bar = 100 μm. (c) Western blot analysis showing expression of reprogramming factors in CM DG cell lines. (d) RT-PCR analysis showing the expression of endogenous or exogenous reprogramming factors in CM DGs. Cj11 (CM embryonic stem cell line) was used as control.

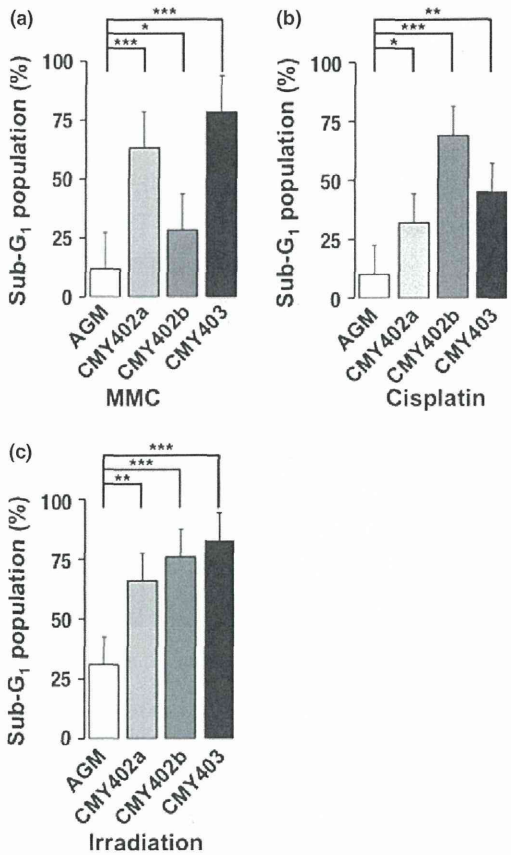

Fig. 4. Effects of DNA-damaging agents and irradiation on common marmoset dysgerminoma-like cells (CM DGs). The cells were treated with (a) mitomycin C (MMC), (b) cisplatin, or (c) irradiation, and the proportions of sub-G_1 populations in aorta-gonado-mesonephros (AGM) fibroblasts or CM DG cell lines were analyzed by FACS. Results are shown as means ± SD. $*P < 0.05$; $**P < 0.01$; $***P < 0.001$.

more sensitive to DNA damage than their parental AGM fibroblasts.

We carried out inverse PCR analyses to identify the integration sites of the lentiviral vectors expressing reprogramming factors in CM DGs. OCT 3/4-, SOX2-, KLF4-, and c-MYC-expressing lentiviral vectors were integrated into 5, 12, 5, and 9 genomic sites, respectively (Fig. S6b, Table S1). The possibility that multiple integrations of lentiviral vectors into the genome caused chromosome instability, leading to the formation of CM DGs, could therefore not be excluded.

Dependence of CM DGs growth on c-MYC and bFGF signalings. To address the question of whether proliferation of CM DGs was dependent on reprogramming factors, we observed the proliferation rate after suppression of each reprogramming factor by shRNA (Fig. S10). Suppression of c-MYC or all four reprogramming factors greatly inhibited the proliferation of CM DGs, indicating that the growth of CM DGs was highly dependent on c-MYC (Fig. 5a).

The proliferation of human ESCs is known to be promoted by bFGF signaling.[23] We examined the possibility that the growth of CM DGs might also be enhanced by bFGF signaling by analyzing the proliferation of CM DGs cultured in medium with or without bFGF. The growth of CM DGs was highly dependent on bFGF (Fig. 5b). Consistent with these results, BGJ398, an inhibitor for FGFR 1 to 4, remarkably inhibited the growth of CM DGs in a dose-dependent manner (Fig. 5c). Moreover, FACS analyses revealed that the sub-G_1 population, representing dead cells, was increased in the presence of BGJ398 (Fig. S11). It should be emphasized that the IC_{50} of BGJ398 (59 nM) was lower for CM DGs than for their parental AGM fibroblasts and control CM skin fibroblasts (Fig. 5d), indicating higher sensitivity of CM DGs. These results suggested that the growth of CM DGs was dependent on bFGF signaling, and therefore FGFR inhibitor could be used to control the growth of the reprogramming factor-induced tumor.

Discussion

In this study we investigated the characteristics of ARCs and CM DGs generated in the reprogramming process of CM AGM fibroblasts by Yamanaka factors.

A normal iPSC line of iPS A cells, showed the expression of ES markers, pluripotency, and flattened morphology, like human iPSCs.[20] In contrast, ARCs showed sphere-like structures, like mouse iPSCs.[1] This morphological difference between iPS A cells and ARCs might be useful to select "true" iPSCs derived from CM, although the underlying molecular mechanisms responsible for this morphological difference remain unknown.

We found, by microarray analyses, that the gene expression pattern in ARCs was more similar to that in iPS A cells than that in AGM fibroblasts, suggesting that reprogramming processes have been done in ARCs by the transduction of reprogramming factors. We also found that genes such as *ZFHX4*, *NFIX*, *HOXC8*, *STMN2*, and *CXORF67* were highly expressed in ARCs. It should be noted that, among these, *HOXC8* is known to be a transcriptional factor related to tumorigenesis.[24] Therefore, these candidates of markers might be useful to predict the tumorigenic potential of iPSCs. Further evaluation is required to confirm our hypothesis.

The original AGM fibroblasts had an abnormal marker chromosome (mar; Fig. 2a, left panel). Although tumor formation was not evident caused in SCID mice (data not shown), this chromosome instability might also be one of the inducers of

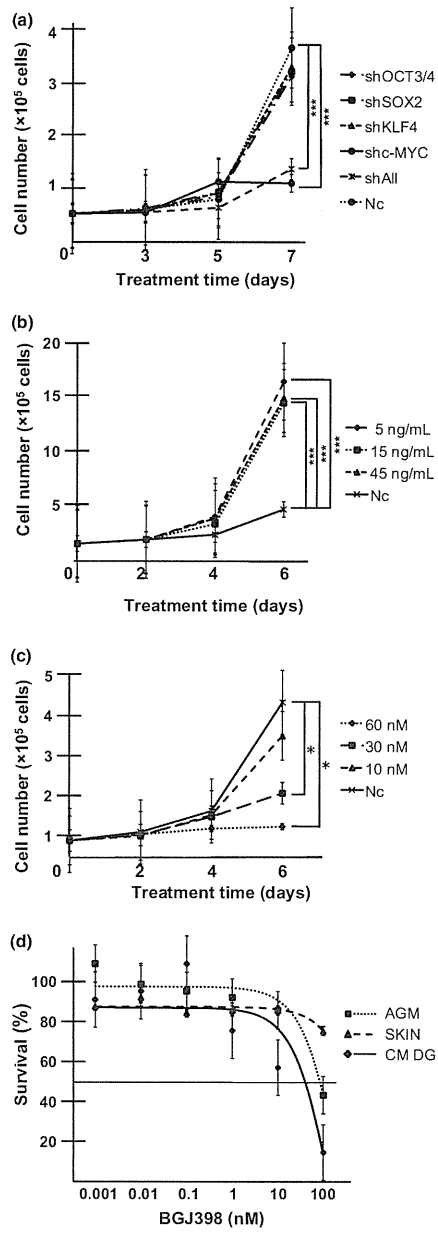

Fig. 5. Dependence of common marmoset dysgerminoma-like (CM DG) cell growth on c-MYC and basic fibroblast growth factor (bFGF) signaling. (a) Inhibition of CM DG growth by knockdown of c-MYC. Cells (3×10^4) were seeded on 24-well plates and transduced with shRNA targeting OCT3/4, SOX2, KLF4, c-MYC, or all reprogramming factors (shAll). Cell growth curves were analyzed by cell counts at the indicated time points. Results are shown as means ± SD. ***$P < 0.001$. Nc, negative control (mock vector). (b) Growth rate of CM DGs was promoted by the addition of bFGF. Cells were cultured in the presence or absence (Nc) of bFGF. Cell numbers were counted at the indicated time points. Results are shown as means ± SD. ***$P < 0.001$. (c) FGFR inhibitor suppressed CM DG growth. Cells were cultured in the presence or absence (Nc) of the FGFR1-4 inhibitor BGJ398; bFGF was added at 5 ng/mL. Cell numbers were counted at the indicated time points. Results are shown as means ± SD. *$P < 0.05$. (d) CM DGs, aorta-gonado-mesonephros fibroblasts (AGM), and CM skin fibroblasts (SKIN) were treated with different concentrations of BGJ398 for 3 days, and the growth-inhibitory effects were analyzed by MTS assay. The IC_{50} for CM DGs was lower than those for parental AGM fibroblasts and control CM skin fibroblasts. Results are shown as means ± SD.

carcinogenesis during the reprogramming process. Thus, needless to say, to generate "safe" iPSCs, validation of the karyotype of the original cells is needed. Moreover, ARCs lost chromosome 4q and X or Y, and possessed an abnormal marker chromosome (mar). Various tumor suppressors including human tumor suppressor gene 1, large tumor suppressor 1 and P36 transformed follicular lymphoma gene have been identified on chromosome 4q in CM cells (Table S2), suggesting that loss of these tumor suppressors might have induced the transformation of CM AGM fibroblasts during reprogramming, although the possibility that translocation of chromosome 4q occurred during the reprogramming process caused the transformation of cells could not be excluded.

It is also possible that the continuous activation of ectopically-transduced transcription factors, including the oncogene *c-MYC*, might have contributed to cell transformation, as described previously.[25,26] Indeed, CM DGs overexpressed c-MYC, and their growth was highly dependent on c-MYC expression, suggesting that downregulation of c-MYC might represent a possible strategy for inhibiting the growth of reprogramming factor-related tumors.

Insertional mutation caused by the integration of lentiviral vectors into the genome might also have promoted cell transformation. Lentiviral vectors expressing reprogramming factors were integrated into at least 31 different genomic sites in CM DGs, some of which were in the vicinity of protein-encoding genes. Moreover, the expression of reprogramming factors transduced by lentiviral vectors continued for over a year in ARCs (data not shown). A safer method, without genome integration, is therefore required for the delivery of reprogramming factors to somatic cells to generate iPSCs applicable for transplantation therapies. Although Sendai virus vectors or transfection of DNA or mRNA may be safer methods,[27] these are lengthy processes that can take more than 1 month to obtain iPSCs,[28] which could also cause stress and lead to genomic instability and subsequent tumor formation. More sophisticated, safer, and more rapid methods of reprogramming might be desirable.

Common marmoset DGs resembled human dysgerminomas in terms of both their pathology and sensitivity to irradiation and DNA-damaging agents.[21,22] In addition, the growth of CM DGs was significantly inhibited by an FGFR1-4 inhibitor. Therefore irradiation, chemotherapy, and FGFR1-4 inhibitors might be effective strategies for controlling human dysgerminomas, and also for tumors that develop in patients treated with iPSC-based therapies.

Acknowledgments

We thank Hiroyuki Miyoshi (Riken, Tsukuba, Japan) for providing lentiviral vectors, Norihiko Kinoshita (Kyushu University, Fukuoka, Japan) and the Laboratory for Technical Support (Medical Institute of Bioregulation, Kyushu University) for their technical assistance, Michiko Ushijima for administrative assistance, and members of Prof. Kenzaburo Tani's laboratory for constructive criticisms. This work was supported by grants from the Project for Realization of Regenerative Medicine (K.T., 08008010) and Kakenhi (T.M., 23590465) from the Ministry of Education, Culture, Sports, Science and Technology, Japan.

Disclosure Statement

The authors have no conflicts of interest.

Abbreviations

AGM	aorta-gonado-mesonephros
AP	alkaline phosphatase
ARC	abnormally reprogrammed cell
bFGF	basic fibroblast growth factor
CM	common marmoset
DG	human dysgerminoma-like cell
ESC	embryonic stem cell
FGFR	fibroblast growth factor receptor
iPSC	induced pluripotent stem cell
K	KLF4
M	c-MYC
MMC	mitomycin C
O	OCT3/4
S	SOX2

References

1 Takahashi K, Yamanaka S. Induction of pluripotent stem cells from mouse embryonic and adult fibroblast cultures by defined factors. *Cell* 2006; **126**: 663–76.
2 Okita K, Yamanaka S. Induced pluripotent stem cells: opportunities and challenges. *Philos Trans R Soc Lond B Biol Sci* 2011; **366**: 2198–207.
3 Okita K, Ichisaka T, Yamanaka S. Generation of germline-competent induced pluripotent stem cells. *Nature* 2007; **448**: 313–U1.
4 Ohm JE, Mali P, Van Neste L *et al.* Cancer-related epigenome changes associated with reprogramming to induced pluripotent stem cells. *Cancer Res* 2010; **70**: 7662–73.
5 Wernig M, Meissner A, Cassady JP, Jaenisch R. c-Myc is dispensable for direct reprogramming of mouse fibroblasts. *Cell Stem Cell* 2008; **2**: 10–2.
6 Okita K, Nakagawa M, Hong HJ, Ichisaka T, Yamanaka S. Generation of mouse induced pluripotent stem cells without viral vectors. *Science* 2008; **322**: 949–53.
7 Judson RL, Babiarz JE, Venere M, Blelloch R. Embryonic stem cell-specific microRNAs promote induced pluripotency. *Nat Biotechnol* 2009; **27**: 459–61.
8 Lin TX, Ambasudhan R, Yuan X *et al.* A chemical platform for improved induction of human iPSCs. *Nat Methods* 2009; **6**: 805–U24.
9 Madonna R. Human-induced pluripotent stem cells. in quest of clinical applications. *Mol Biotechnol* 2012; **52**: 193–203.
10 Lunn SF. Systems for collection of urine in the captive common marmoset, *Callithrix-Jacchus*. *Lab Anim* 1989; **23**: 353–6.
11 Marumoto T, Tashiro A, Friedmann-Morvinski D *et al.* Development of a novel mouse glioma model using lentiviral vectors. *Nat Med* 2009; **15**: 110–6.
12 Tomioka I, Maeda T, Shimada H *et al.* Generating induced pluripotent stem cells from common marmoset (*Callithrix jacchus*) fetal liver cells using defined factors, including Lin28. *Genes Cells* 2010; **15**: 959–69.
13 Foster KW, Frost AR, McKie-Bell P *et al.* Increase of GKLF messenger RNA and protein expression during progression of breast cancer. *Cancer Res* 2000; **60**: 6488–95.
14 Gustafson WC, Weiss WA. Myc proteins as therapeutic targets. *Oncogene* 2010; **29**: 1249–59.
15 Vogelstein B. Genetic instabilities in human cancers. *Biophys J* 1999; **76**: A135–A.
16 Sasaki E, Hanazawa K, Kurita R *et al.* Establishment of novel embryonic stem cell lines derived from the common marmoset (*Callithrix jacchus*). *Stem Cells* 2005; **23**: 1304–13.
17 Li XJ, Du ZW, Zarnowska ED *et al.* Specification of motoneurons from human embryonic stem cells. *Nat Biotechnol* 2005; **23**: 215–21.
18 Liao JY, Marumoto T, Yamaguchi S *et al.* Inhibition of PTEN tumor suppressor promotes the generation of induced pluripotent stem cells. *Mol Ther* 2013; **21**: 1242–50.
19 Tumor of the ovary, Maldeveloped Gonads, Fallopian tube, and Broad Ligament., 1998; 239–65.
20 Ulbright TM. Germ cell tumors of the gonads: a selective review emphasizing problems in differential diagnosis, newly appreciated, and controversial issues. *Mod Pathol* 2005; **18** (Suppl 2): S61–79.

21 Brewer M, Gershenson DM, Herzog CE, Mitchell MF, Silva EG, Wharton JT. Outcome and reproductive function after chemotherapy for ovarian dysgerminoma. *J Clin Oncol* 1999; **17**: 2670–5.
22 Thoeny RH, Dockerty MB, Hunt AB, Childs DS Jr. A study of ovarian dysgerminoma with emphasis on the role of radiation therapy. *Surg Gynecol Obstet* 1961; **113**: 692–8.
23 Bendall SC, Stewart MH, Menendez P *et al.* IGF and FGF cooperatively establish the regulatory stem cell niche of pluripotent human cells in vitro. *Nature* 2007; **448**: 1015–U3.
24 Li Y. HOXC8-dependent cadherin 11 expression facilitates breast cancer cell migration through trio and rac. *Genes Cancer* 2011; **2**: 880–8.
25 Nakagawa M, Koyanagi M, Tanabe K *et al.* Generation of induced pluripotent stem cells without Myc from mouse and human fibroblasts. *Nat Biotechnol* 2008; **26**: 101–6.
26 Gordan JD, Thompson CB, Simon MC. HIF and c-Myc: sibling rivals for control of cancer cell metabolism and proliferation. *Cancer Cell* 2007; **12**: 108–13.
27 Seki T, Yuasa S, Fukuda K. Derivation of induced pluripotent stem cells from human peripheral circulating T cells. *Curr Protoc Stem Cell Biol* 2011; 11–14. Chapter 4: Unit4A.3.
28 Buganim Y, Faddah DA, Cheng AW *et al.* Single-cell expression analyses during cellular reprogramming reveal an early stochastic and a late hierarchic phase. *Cell* 2012; **150**: 1209–22.

Supporting Information

Additional supporting information may be found in the online version of this article:

Fig. S1. Expression of embryonic stem cell (ESC) markers in abnormally reprogrammed cells (ARCs).

Fig. S2. Impaired differentiation of abnormally reprogrammed cells (ARCs).

Fig. S3. Expression of c-KIT, CD30, and CD45 in common marmoset dysgerminoma-like cells.

Fig. S4. Colony formation of aorta-gonado-mesonephros fibroblasts by the transduction of OCT3/4, SOX2, KLF4, and c-MYC (OSKM) and OSM.

Fig. S5. Validation of genes showing upregulation in abnormally reprogrammed cells (ARCs) compared to normal induced pluripotent stem (iPS) A cells in microarray analysis.

Fig. S6. Integration of reprogramming genes into the genome of common marmoset dysgerminoma-like cells (CM DGs).

Fig. S7. Fluorescence-activated cell sorter analyses to reveal effects of mitomycin C treatment on common marmoset dysgerminoma-like cell lines.

Fig. S8. Fluorescence-activated cell sorter analyses to reveal effects of cisplatin treatment on common marmoset dysgerminoma-like cell lines.

Fig. S9. Fluorescence-activated cell sorter analyses to reveal effects of irradiation on common marmoset dysgerminoma-like cell lines.

Fig. S10. Knockdown of OCT3/4, SOX2, KLF4, or c-MYC by shRNA in common marmoset dysgerminoma-like cell lines.

Fig. S11. Induction of cell death in common marmoset dysgerminoma-like cells by BGJ398.

Table S1. Lentiviral vector integration sites in common marmoset (CM) dysgerminoma-like cells.

Table S2. Human homologs of candidate tumor suppressors located on chromosome 4q in common marmoset (CM).

Video S1. *In vitro* differentiation assay to assess the ability of abnormally reprogrammed cells to differentiate into cardiomyocytes.

Data S1. Materials and Methods.

FEBS Open Bio 4 (2014) 213–219

ELSEVIER

FEBS openbio

journal homepage: www.elsevier.com/locate/febsopenbio

Analysis of essential pathways for self-renewal in common marmoset embryonic stem cells

Takenobu Nii[a,1], Tomotoshi Marumoto[a,b,1], Hirotaka Kawano[a], Saori Yamaguchi[a], Jiyuan Liao[a], Michiyo Okada[a], Erika Sasaki[c,d], Yoshie Miura[a], Kenzaburo Tani[a,b,*]

[a] Division of Molecular and Clinical Genetics, Medical Institute of Bioregulation, Kyushu University, 3-1-1, Maidashi, Higashi-ku, Fukuoka 812-8582, Japan
[b] Department of Advanced Molecular and Cell Therapy, Kyushu University Hospital, 3-1-1, Maidashi, Higashi-ku, Fukuoka 812-8582, Japan
[c] Central Institute for Experimental Animals, Kawasaki, Kanagawa 216-0001, Japan
[d] Keio Advanced Research Center, Keio University School of Medicine, Tokyo 160-8582, Japan

ARTICLE INFO

Article history:
Received 21 November 2013
Revised 12 February 2014
Accepted 12 February 2014

Keywords:
Embryonic stem cells
Common marmoset
bFGF
TGFβ
Self-renewal

ABSTRACT

Common marmoset (CM) is widely recognized as a useful non-human primate for disease modeling and preclinical studies. Thus, embryonic stem cells (ESCs) derived from CM have potential as an appropriate cell source to test human regenerative medicine using human ESCs. CM ESCs have been established by us and other groups, and can be cultured *in vitro*. However, the growth factors and downstream pathways for self-renewal of CM ESCs are largely unknown. In this study, we found that basic fibroblast growth factor (bFGF) rather than leukemia inhibitory factor (LIF) promoted CM ESC self-renewal via the activation of phosphatidylinositol-3-kinase (PI3K)-protein kinase B (AKT) pathway on mouse embryonic fibroblast (MEF) feeders. Moreover, bFGF and transforming growth factor β (TGFβ) signaling pathways cooperatively maintained the undifferentiated state of CM ESCs under feeder-free condition. Our findings may improve the culture techniques of CM ESCs and facilitate their use as a preclinical experimental resource for human regenerative medicine.

1. Introduction

Human regenerative medicine, including transplantation of various functional cells differentiated from embryonic stem cells (ESCs) or induced pluripotent stem cells (iPSCs), is considered to have great potential for treating various incurable diseases, and has thus attracted much public attention. However, preclinical studies using animal disease models are required to evaluate the efficacy and safety of ESC/iPSC-derived cells prior to their clinical application. Common marmoset (CM, *Callithrixjacchus*) has recently been recognized as a useful non-human primate for such studies, because of its small size, high reproductive capacity, and genetic similarity to humans [1].

Understanding the molecular mechanisms governing the self-renewal of ESCs is important for the development of technologies to differentiate them into functional cells. Although both human and mouse ESCs are able to self-renew on feeder cells in vitro, their growth factor requirements for self-renewal are different. Basic fibroblast growth factor (bFGF), which activates phosphatidylinositol-3-kinase (PI3K)-protein kinase B (AKT) [2,3] and mitogen-activated protein/extracellular signal-regulated kinase kinase (MEK)-extracellular signal-regulated kinase (ERK) pathways [2–8], and transforming growth factor β (TGFβ) leading to the activation of mothers against decapentaplegic homolog 2/3 (SMAD2/3) [2,6–11], maintain the self-renewal of human ESCs and mouse epiblast stem cells (EpiSCs). Conversely, in mouse ESCs, leukemia inhibitory factor (LIF), which activates janus kinase (JAK)-signal transducer and activator of transcription 3 (STAT3) and PI3K-AKT pathways, is known to play important roles in maintaining self-renewal [12–14].

Abbreviations: AKT, protein kinase B; bFGF, basic fibroblast growth factor; CM, common marmoset; EB, embryoid body; EpiSCs, epiblast stem cells; ERK, extracellular signal-regulated kinase; ESCs, embryonic stem cells; FCM, flow cytometry; iPSCs, induced pluripotent stem cells; JAK, janus kinase; KSR, knockout serum replacement; LIF, leukemia inhibitory factor; MEFs, mouse embryonic fibroblasts; MEK, mitogen-activated protein/extracellular signal-regulated kinase kinase; PI3K, phosphatidylinositol-3-kinase; RT-PCR, reverse transcription-polymerase chain reaction; SMAD2/3, mothers against decapentaplegic homolog 2/3; STAT3, signal transducer and activator of transcription 3; TGFβ, transforming growth factor β

* Corresponding author at: Division of Molecular and Clinical Genetics, Medical Institute of Bioregulation, Kyushu University, 3-1-1, Maidashi, Higashi-ku, Fukuoka 812-8582, Japan. Tel.: +81 92 642 6434; fax: +81 92 642 6444.
E-mail address: taniken@bioreg.kyushu-u.ac.jp (K. Tani).

[1] The first two authors contributed equally to this work.

http://dx.doi.org/10.1016/j.fob.2014.02.007

ESCs derived from CM have been established by us and others [15–17]. However, the growth factors used in the culture medium are different among reports [15,17–21]. Thus, the most appropriate growth factor and its downstream pathway for maintaining the self-renewal of CM ESCs still remain to be determined.

In the present study, we characterized two CM ESC cell lines, Cj11 and CM40, and found that CM ESCs were more similar to human ESCs rather than mouse ESCs in terms of their growth factor requirement and molecular signaling pathways for self-renewal.

2. Materials and methods

2.1. CM ESC culture on mouse embryonic fibroblasts (MEFs)

CM ESC lines, CM40 and Cj11, were maintained in CM ESC medium as described before [15] with or without 1:1000 LIF (Wako, Osaka, Japan), 5 ng/ml bFGF (PeproTech, NJ, USA), 5 μM PD0325901 (MEK inhibitor, Wako) or 10 μM LY294002 (PI3K inhibitor, Santa Cruz Biotechnology, CA, USA). CM40 cell line was established in our laboratory [15], and Cj11 cell line was obtained from WiCell Research Institute [16]. MEFs were prepared from 13.5 dpc embryos from ICR mice (Charles River, Japan) using established procedures [22].

2.2. CM ESC culture under feeder-free conditions

CM40 and Cj11 ESC lines were cultured on Matrigel (BD Biosciences, CA, USA)-coated dishes in Essential 8 medium (Life Technologies, NY, USA) or Essential 6 medium (Life Technologies) with or without 1:1000 LIF (Wako), 100 ng/ml bFGF (PeproTech), 2 ng/ml TGFβ (PeproTech), 5 μM PD0325901 (MEK inhibitor, Wako), 10 μM LY294002 (Santa Cruz Biotechnology).

2.3. CM ESC differentiation

Undifferentiated ESCs were detached from the feeder cells by treatment with 0.25% trypsin (NacalaiTesque, Kyoto, Japan) for 1 min. The collected colonies were processed for embryoid body (EB) formation assay in CM ESC medium on low cell-binding 12-well plates (Nalge Nunc International KK, Japan) for 4 or 8 days. Detailed protocols to differentiate CM ESCs into three germ layers are described in "Supplementary Materials and Methods".

2.4. Immunocytochemistry

Cells were fixed in 4% paraformaldehyde (PFA)/phosphate-buffered saline (PBS) (NacalaiTesque), permeabilized with 0.3% Triton X-100/PBS, blocked with staining buffer (2% fetal bovine serum (FBS)/PBS). The primary antibodies used are shown in Supplementary Table 1. Nuclei were counterstained with DAPI. Images were obtained under a fluorescence microscope (Axiovert 135M; Carl Zeiss, Germany, or BZ-9000; Keyence) and then analyzed by Axiovert software (Carl Zeiss) or BZ-Analyzer software (Keyence).

2.5. Flow cytometry (FCM)

CM ESCs were fixed in 4% PFA/PBS, permeabilized with 0.3% Triton X-100/PBS, blocked with staining buffer (2% FBS/PBS), and then incubated with an anti-OCT3/4 antibody (Santa Cruz Biotechnology, sc-5279 or sc-8628). The cells were detected on a FACSVerse flow cytometer (Becton Dickinson, USA), followed by data analysis using FlowJo software (Tomy Digital Biology, Japan).

2.6. Reverse transcription-polymerase chain reaction (RT-PCR)

Total RNA was isolated using an RNeasy Mini Kit (Qiagen, USA), and cDNA was synthesized using Superscript III reverse transcriptase (Life Technologies). Then PCR was carried out using the synthesized cDNA as templates and gene-specific primers (see Supplemental Table 2). The primers were designed based on different exons to span the intervening intron and avoid amplification of contaminating genomic DNA.

2.7. Western blotting

Cells were incubated on ice with RIPA buffer containing protease inhibitors (Complete Mini, EDTA-free; Roche, Basel, Switzerland) and a phosphatase inhibitor cocktail (NacalaiTesque). The cell lysates were then resolved by SDS-polyacrylamide gel electrophoresis, followed by immunoblotting. The primary antibodies used are shown in Supplementary Table 3. The signals were detected using a LAS3000 (Fujifilm, Japan). Band intensities were measured by ImageJ software (NIH).

2.8. Statistical analysis

Unless otherwise noted, inter-group differences were analyzed using analysis of variance (ANOVA) followed by the Tukey's post-hoc test with GraphPad Prism 5 (GraphPad Software, CA, USA).

3. Results

3.1. bFGF promotes self-renewal of CM ESCs on feeder cells

bFGF and LIF have been reported to be essential for the maintenance of human and mouse ESCs, respectively [3,12–14,23–27], and either or both of these growth factors were considered to be required for the maintenance of CM ESCs. To determine the optimal condition for culturing CM ESCs, we first examined the expression of receptors for bFGF (FGFR1, FGFR2, FGFR3, and FGFR4) and LIF (LIFR and gp130). RT-PCR analysis demonstrated that all of these receptors were expressed in the CM ESCs (Fig. 1A), suggesting that both growth factors play important roles in the biology of CM ESCs.

In culture, ESCs are generally known to spontaneously differentiate. However, the addition of appropriate growth factors inhibits such spontaneous differentiation. To evaluate the effects of bFGF and LIF on the proliferation and differentiation of CM ESCs in vitro, we passaged CM ESCs at a ratio of 1:3 every three days for three passages, and then counted the numbers of undifferentiated OCT3/4$^+$ cells. We found that the proportion of OCT3/4$^+$ cells was unchanged regardless of the addition of bFGF or LIF (Fig. 1B). However, the numbers of OCT3/4$^+$ cells were significantly increased by the addition of bFGF, but not LIF, compared with those of controls cultured without bFGF and LIF (Fig. 1C). Similar results were obtained when the cells were cultured for more than ten passages (Supplementary Fig. S1 and data not shown). The above experiments were performed using CM40 cell line, and similar results were obtained with Cj11 cell line (Supplementary Fig. S2). These results strongly suggest that bFGF promotes the proliferation of CM ESCs rather than maintaining the undifferentiated state of CM ESCs.

3.2. bFGF-PI3K-AKT pathway supports self-renewal of CM ESCs on feeder cells

bFGF and its downstream PI3K-AKT and MEK-ERK pathways are important for the self-renewal of human ESCs [2,3,5,6]. We therefore examined whether these pathways were activated by bFGF for CM ESC self-renewal on feeder cells. CM ESCs were cultured overnight in medium lacking knockout serum replacement (KSR) and any growth factors. Then, we added bFGF (5 ng/ml), and examined the activation of AKT and ERK1/2 in the cells by Western blotting.

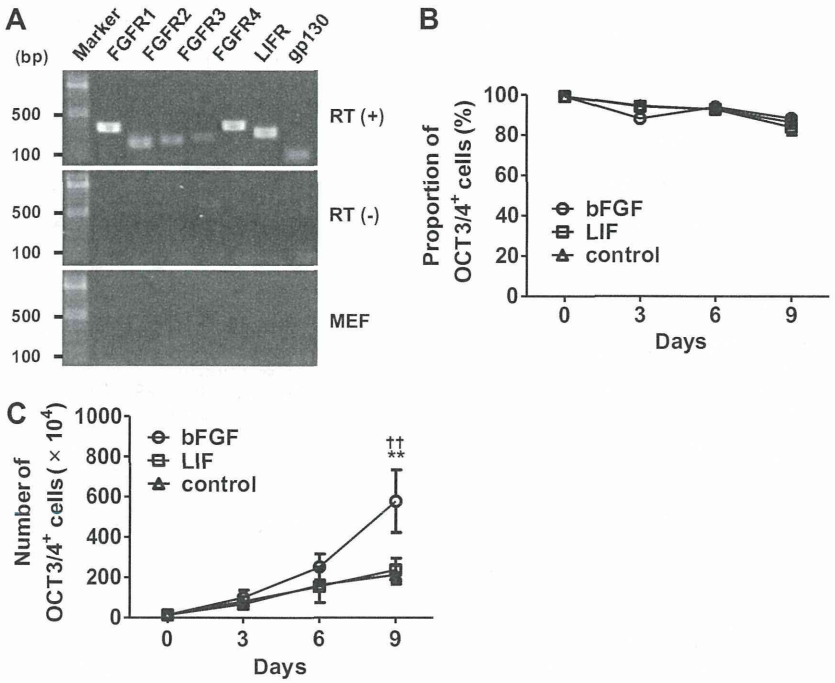

Fig. 1. bFGF promotes self-renewal of CM ESCs in the presence of feeder support. (A) RT-PCR analysis showing the expression of FGFR1, FGFR2, FGFR3, FGFR4, LIFR, and gp130 genes in CM ESCs (CM40). (B) No effect of bFGF on the proportion of OCT3/4$^+$ cells. CM ESCs (CM40; 1.4 × 10^5) were seeded on mitomycin C (MMC)-treated MEFs and cultured with LIF (open square), bFGF (open circle), or without growth factors (control; open triangle). The percentage of OCT3/4$^+$ cells was determined by FCM. (C) Enhancement of undifferentiated CM ESC growth by bFGF. CM ESCs (CM40; 1.4 × 10^5) were seeded on mitomycin C (MMC)-treated MEFs and cultured with LIF (open square), bFGF (open circle), or without growth factors (control; open triangle). The number of cells was then counted by trypan blue exclusion. The number of OCT3/4$^+$ cells was determined by multiplying the number of cells by the percentage of OCT3/4$^+$ cells and the passage ratio together. Data are shown as the mean ± SD (n = 4). $^{**}P < 0.01$ (bFGF vs. control) and $^{\dagger\dagger}P < 0.01$ (bFGF vs. LIF). Note that all of PCR in (A) was performed with 30 cycles, and no bands were detected for FGFR expression in MEFs in (A), however, they were faintly done when PCR was performed with 40 cycles.

The results showed that the band intensity of phosphorylated AKT was significantly increased after the treatment with bFGF, while that of phosphorylated ERK1/2 was not changed (Fig. 2A and B). These data suggested that PI3K-AKT, but not MEK-ERK, pathway was activated by bFGF in CM ESCs under feeder-dependent culture condition.

Next, to examine whether bFGF-PI3K-AKT pathway plays any roles in the maintenance of self-renewal of CM ESCs, the cells were cultured in medium containing bFGF in the presence or absence of the PI3K inhibitor, LY294002. We found that the proportion of OCT3/4$^+$ cells was maintained at approximately 90% for at least three passages when the cells were cultured without LY294002, whereas it was gradually decreased when the cells were cultured with LY294002 (day0, 96.75 ± 2.83% vs. day9, 57.97 ± 16.76%, Fig. 2C). In addition, OCT3/4$^+$ cell proliferation was inhibited in the presence of LY294002 (day9, bFGF, 7.61 ± 1.59×10^6 cells vs. bFGF+LY294002, 2.36 ± 1.25×10^6 cells, Fig. 2D). Additionally, even when bFGF was not added, the proportion of OCT3/4$^+$ cells was significantly reduced by the treatment with LY294002 (Fig. 2C), indicating that PI3K-AKT pathway is activated by unknown factors from MEFs and play roles for self-renewal of CM ESCs. Overall, these results strongly suggest that bFGF-PI3K-AKT pathway is essential for the self-renewal of CM ESCs under feeder-dependent culture condition.

To examine the expression of OCT3/4, we used an antibody against amino acids 1–134 of human OCT3/4 (monoclonal OCT3/4 antibody, sc-5279) that was known to be useful for detecting the expression of CM OCT3/4 [28]. And recent study reported that another antibody raised against amino acids 1–19 of human OCT3/4 (polyclonal OCT3/4 antibody, sc-8628) was more useful to detect ESC-specific OCT3/4 [29]. Thus we performed immunocytochemistry and FCM analysis using sc-8628, and obtained the similar results (Supplementary Fig. S3).

3.3. bFGF and TGFβ signaling cooperate to maintain the undifferentiated state of CM ESCs under feeder-free conditions

All of the experiments described above were performed with feeder support. Thus, the various secreted factors including cytokines and adhesion molecules might have affected the results. To examine the dependency of CM ESCs on feeder cells, CM ESCs were cultured on a high or low density of feeder cells, and then the undifferentiated state was examined by immunocytochemistry using an anti-NANOG antibody (Supplementary Fig. S1). We found that CM ESCs on low-density feeder cells lost their expression of NANOG after four passages, whereas those on high-density feeder cells maintained NANOG expression even after ten passages (Supplementary Fig. S1). Therefore, it is conceivable that the self-renewal of CM ESCs is maintained by unknown factors derived from feeder cells.

Chen et al. showed that Essential 8 medium (Dulbecco's modified Eagle's medium/F12 supplemented with L-ascorbic acid-2-phosphate magnesium, insulin, transferrin, sodium selenium, $NaHCO_3$, bFGF, and TGFβ) supports the self-renewal of human ESCs and iPSCs under feeder-free conditions [30]. To clarify the essential growth factors required for maintaining the undifferentiated state of CM ESCs, CM ESCs were cultured under feeder-free condition. We found that CM ESCs could be cultured on Matrigel in Essential 8 medium without feeder support, although they could not be maintained for more than three passages (data not shown). Next, we cultured CM ESCs on Matrigel in Essential 6 medium lacking bFGF and TGFβ overnight, and then the activation of signaling

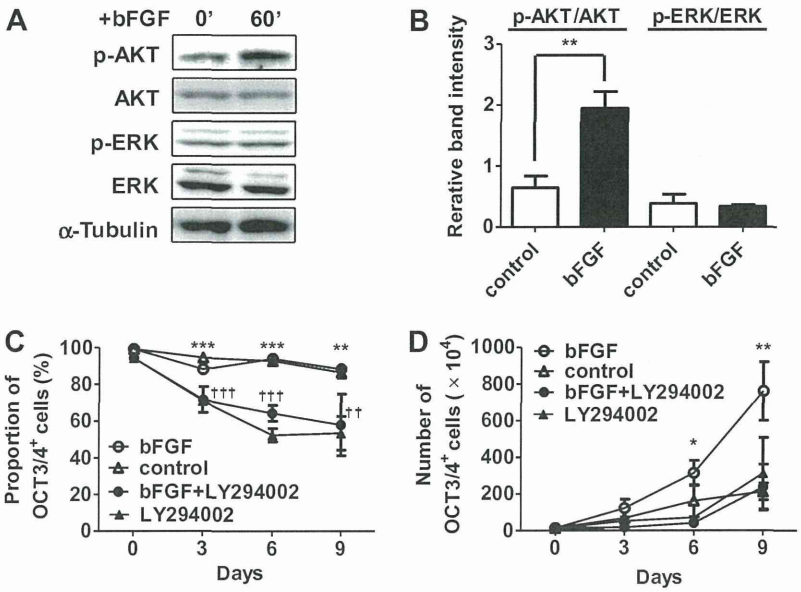

Fig. 2. bFGF-PI3K-AKT pathway supports self-renewal of CM ESCs. (A) Western blot analysis showing the activation of AKT by bFGF in CM ESCs. CM40 cells were starved of bFGF and KSR overnight, and then stimulated with 5 ng/ml of bFGF for the indicated durations. AKT, ERK1/2 and α-Tubulin are shown as loading controls. The relative band intensities of p-AKT/AKT and p-ERK/ERK are shown in (B). Band intensities were measured by ImageJ software. Data are shown as the mean ± SD. The Student's *t*-test was used to test inter-group differences. $^{**}P < 0.01$. (C) Inhibition of self-renewal by LY294002. CM ESCs (CM40; 1.4×10^5) were seeded on MMC-treated MEFs and cultured in medium containing bFGF (open circle), control medium (open triangle), bFGF+LY294002 (closed circle) or LY294002 (closed triangle). The percentage of OCT3/4$^+$ cells was then determined by FCM at the indicated day as shown in (C). The number of live cells was counted by trypan blue exclusion. Growth curves were generated by multiplying the number of live cells by the percentage of OCT3/4$^+$ cells and passage ratio together as shown in (D). Data are shown as the mean ± SD. bFGF, $n = 4$; control, $n = 4$; bFGF+LY294002, $n = 3$; LY294002, $n = 3$; $^{*}P < 0.05$, $^{**}P < 0.01$, and $^{***}P < 0.005$, bFGF vs. control; $^{\dagger\dagger}P < 0.01$ and $^{\dagger\dagger\dagger}P < 0.005$, bFGF+LY294002 or LY294002 vs. control.

pathways known to maintain mouse and human ESCs (bFGF-PI3K-AKT, bFGF-MEK-ERK, TGFβ-SMAD2/3, and LIF-JAK-STAT3 pathways) were analyzed by Western blotting after the addition of bFGF, TGFβ, or LIF to the medium. We found that phosphorylation of AKT and ERK was increased by the addition of bFGF, while it was decreased by the treatment with LY294002 or PD0325901, suggesting that both of AKT and ERK were activated downstream of bFGF under feeder-free condition (Fig. 3A and B). And the addition of TGFβ resulted in an increase of phosphorylated SMAD2/3 (Fig. 3A and B), suggesting that SMAD2/3 was activated downstream of TGFβ. Moreover, the addition of LIF resulted in an increase of phosphorylated STAT3, suggesting that STAT3 was activated downstream of LIF (Supplementary Figs. S4B and D). These results suggested that bFGF-PI3K-AKT, bFGF-MEK-ERK, TGFβ-SMAD2/3 and LIF-JAK-STAT3 pathways known to regulate self-renewal of human or mouse ESCs were activated in CM ESCs under feeder-free condition. It should be noted that ERK was not activated by 5 ng/ml of bFGF that was used for the culture on feeder cells as described in Fig. 2A and B (Supplementary Fig. S4B), but it was remarkably activated by 100 ng/ml of bFGF generally used for feeder-free culture of human ESCs (Fig. 3A and B) [30].

Next, to determine the growth factors maintaining the undifferentiated state of CM ESCs under feeder-free condition, CM ESCs were cultured in the feeder-free system with various combinations of growth factors, followed by analysis of their undifferentiated state morphologically and immunocytochemically. Most of the colonies cultured in Essential 6 medium with bFGF, bFGF+TGFβ, bFGF+LIF, or bFGF+TGFβ+LIF showed a well-packed appearance, and a majority of the cells expressed NANOG (Fig. 3C). In contrast, most of the colonies cultured in Essential 6 medium with TGFβ, LIF, or TGFβ+LIF showed an unpacked appearance, and a majority of the cells did not express NANOG (Fig. 3C). Moreover, NANOG$^+$ and well-packed colonies were found at the highest proportion (98.00 ± 0.88%) when the cells were cultured in the presence of TGFβ+bFGF (Fig. 3D). In addition, almost all of the colonies were positive for OCT3/4, SOX2, SSEA-4, TRA1-60 and TRA1-81 (Supplementary Fig. S3), and these colony forming cells kept the capability of differentiating three lineages (Supplementary Fig. S5). This observation indicates that the addition of both TGFβ and bFGF is the most appropriate growth factor combination for maintenance of the undifferentiated state of CM ESCs under feeder-free condition, which is similar to a characteristic of human ESCs [2,6,9–11].

3.4. CM ESCs show phenotypes similar to those of human ESCs and mouse EpiSCs

Human ESCs and mouse EpiSCs share a number of similar phenotypes as shown in Table 1 [7,8]. CM ESCs formed flattened colonies and expressed NANOG as well as markers for both mouse EpiSCs and human ESCs, such as T, CER1, EOMES, FOXA2, GATA6, and SOX17 (Supplementary Figs. S1 and S6A) [7]. Moreover, bFGF and TGFβ signalings play crucial roles in maintaining the undifferentiated state of human ESCs and mouse EpiSCs [2,7,8,11,30], and the same roles of these signaling pathways were also found in CM ESCs (Fig. 3C and D).

Previous reports have shown that apoptosis of human ESCs and mouse EpiSCs is induced by culturing after complete dissociation [31,32]. Watanabe et al. showed that dissociation-induced apoptosis of human ESCs is suppressed by treatment with the Rho-associated kinase (ROCK) inhibitor Y27632 [33]. To examine whether dissociation-induced apoptosis of human ESCs and mouse EpiSCs was similarly found in CM ESCs, colonies of CM ESCs were dissociated into single cells by trypsinization, and then the cells were plated on Matrigel-coated dishes with or without Y27632. Compared with untreated controls, we found that Y27632-treated CM ESCs produced